https://doi.org/10.5194/egusphere-2026-669
Preprint. Discussion started: 2 March 2026

Modelling the evolution of Thwaites Glacier over the 20th century

David T. Bett[1], Alexander T. Bradley[2], Bertie W.J Miles[3], C. Rosie Williams[1], Paul R. Holland[1] and Robert J. Arthern[1]

[1]British Antarctic Survey, Cambridge, UK
[2]King's College London, London, UK
[3]University of Edinburgh, Edinburgh, UK

Correspondence to: David T. Bett (d.bett@bas.ac.uk)

Abstract.

Thwaites Glacier is rapidly evolving and could make large sea-level contributions in the coming centuries, making it essential to understand the drivers of the ongoing ice loss. Sediment-core analysis suggests that Thwaites Glacier was in a relatively steady state for millennia before its western pinning point ungrounded in the 1940s. Here, we include a first analysis of 1947 aerial imagery of Thwaites Ice Shelf, which shows that it was relatively undamaged, contrasting with the highly-damaged present-day. Additionally, the main outflow and shear margin were displaced ~15km westwards compared to the present day. We use the MITgcm-WAVI coupled ocean-ice sheet model to create example quasi-steady pre-1940s configurations for Thwaites Glacier, including a most plausible pre-1940s state, finding that healing the damaged ice shelf is necessary to achieve this. Next, we trigger ice retreat and highlight key processes as the model evolves into the present-day configuration, including ice damage, pinning-point ungrounding driven by ocean melting, and ice piracy between eastern and western parts of Thwaites Glacier. By conducting reversibility experiments during the retreat, we find that multiple quasi-steady ice-sheet states are possible under the same ocean forcing, demonstrating the potential for tipping points in the Thwaites system. Either ice damage or increased ocean forcing can eliminate these quasi-steady states, prompting retreat resembling that observed today. Taken together, these results demonstrate that the sea-level contribution from Thwaites Glacier is not simply controlled by ocean warming in the Amundsen Sea, and is highly sensitive to ice-damage feedbacks, which must be incorporated into sea-level projections.

https://doi.org/10.5194/egusphere-2026-669
Preprint. Discussion started: 2 March 2026

1. Introduction

The West Antarctic ice sheet is losing mass, with the largest contribution coming from the Amundsen Sea Sector (Shepherd et al., 2018). Within the Amundsen Sector, Thwaites Glacier alone contributed 4% of all global sea level rise between 1993-2017 (Rignot et al., 2019; Shepherd et al., 2019; Cazenave et al., 2018). Since satellite records began in the 1970s, its ice flux has been accelerating (Mouginot et al., 2014), with potential for large but highly uncertain sea level rise in the future (e.g. Arthern and Williams, 2017; Joughin et al., 2014; Seroussi et al., 2020; Yu et al., 2018; Bett et al., 2024).

Over the satellite era, grounding-line retreat has been observed for both the western and eastern parts of Thwaites Glacier (Rignot et al., 2014; Milillo et al., 2019), along with increasing ice-shelf damage, especially on the western ice shelf (Miles et al., 2020), leading to the disintegration of the western ice shelf in the present day (Figure 1b). High melt rates are modelled to occur beneath the western main trunk of the glacier (Holland et al., 2023; Nakayama et al., 2019), but supressed low melt rates have been observed in eastern Thwaites (Davis et al., 2023). Previous studies have suggested that Thwaites Glacier would continue to retreat even with no ice shelf melting at all (Williams et al., 2026; Bett et al., 2024), albeit at a slower (and decelerating) rate compared to the faster (and accelerating) retreat produced by realistic melting (Bett et al., 2024). However, other studies have found that the present-day grounding line of Thwaites Glacier is not inherently unstable when starting from a steady position (Hill et al., 2023) and has yet to pass a tipping point, if the present-day configuration is assumed to be close to equilibrium under cold historical forcings (Reese et al., 2023). Additionally, further modelling work found that the present-day configuration of Thwaites Ice shelf provides minimal buttressing, leading to the conclusion that Thwaites Glacier in the present day is stable but unsteady (Gudmundsson et al., 2023). The state of low buttressing may be an ephemeral situation since new ice rises and rumples will be produced during retreat (Bett et al., 2024).

https://doi.org/10.5194/egusphere-2026-669
Preprint. Discussion started: 2 March 2026

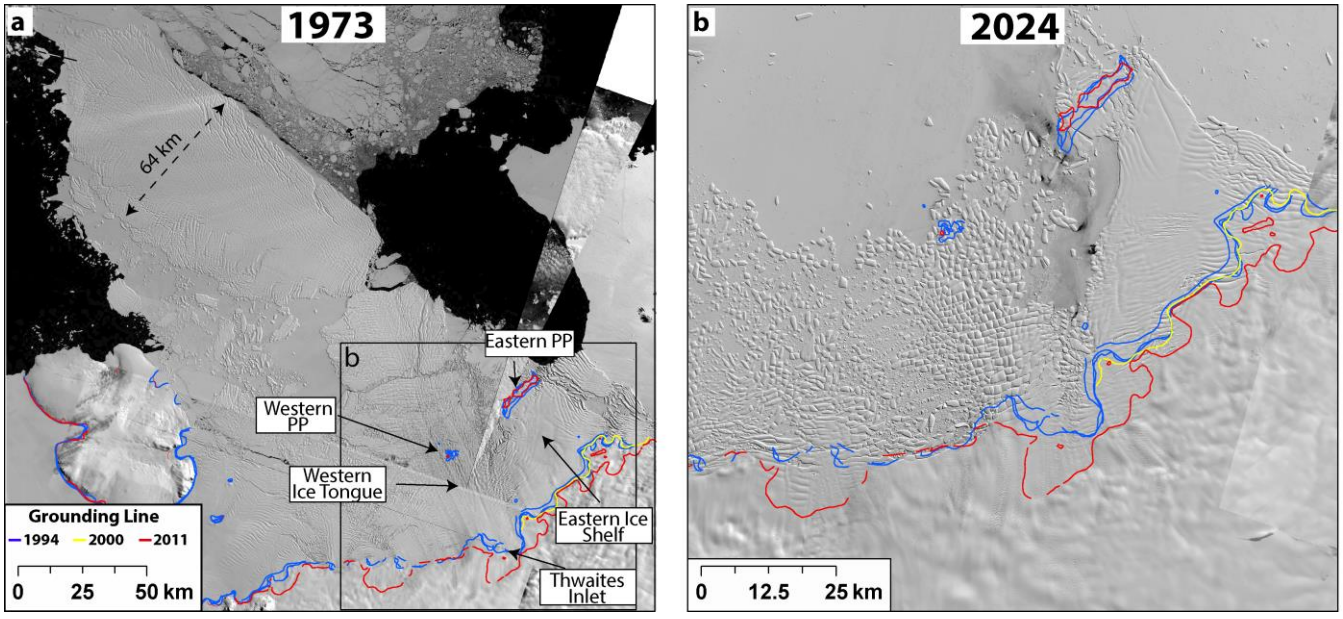

Figure 1: Landsat satellite images of Thwaites Ice Shelf for a) Geo-corrected Landsat-1 image mosaic from 1973 (Miles and Bingham, 2024), and b) Landsat-8 from 2024. Observed grounding lines added for 1994, 2000 and 2011 (Rignot et al., 2016).

A key feature of Thwaites Ice Shelf evolution over the satellite era is an overall progressive increase in damage, effectively reducing the bulk viscosity of the ice, with damage variability additionally occurring within this trend (Lhermitte et al., 2020; Surawy-Stepney et al., 2023). Damage modelling of these complex processes is still in its infancy (e.g. Sun et al., 2017; Clayton et al., 2022) and has not been included in most previous modelling of Thwaites Glacier (e.g. Bett et al., 2024; Arthern and Williams, 2017; Joughin et al., 2014; Yu et al., 2018; Gudmundsson et al., 2023) .

Thwaites Glacier has undergone major changes over the 20th / 21st centuries, with the first satellite image of Thwaites Ice Shelf in 1973 (Miles and Bingham, 2024) (Figure 1a), showing a western Thwaites that is damaged but far more intact than in the present day (Miles et al., 2020) (Figure 1b). Crucially, a key feature of this image is a large intact iceberg near Thwaites western ice shelf, with sketched outlines for 1947 (Ferrigno et al., 1993) and for 1966 (Williams and Carter, 1976) suggesting that this intact iceberg was attached to the western Thwaites Ice Shelf. Such a long and cohesive ice tongue suggests that Thwaites Ice Shelf was relatively undamaged for centuries prior to sometime before the 1973 image. Sediment core analyses suggest that the western pinning point of Thwaites Glacier ungrounded in the 1940s, coinciding with the ungrounding of nearby Pine Island Glacier (Clark et al., 2024; Smith et al., 2017), with possible grounding line retreat occurring in western Thwaites during the 1950s (Clark et al., 2024). Aerial images of Thwaites Ice Shelf were taken in 1947

https://doi.org/10.5194/egusphere-2026-669
Preprint. Discussion started: 2 March 2026

during the U.S. operation Highjump (USGS, 2018) and are analysed and compared to the first satellite image in 1972/3 below in section 2 for the first time, to our knowledge, providing further insight into the configuration of Thwaites Ice Shelf prior to the major changes that ensued.

Changes in oceanic melting are the ultimate cause of Amundsen Sea glaciers' thinning and retreat (Shepherd et al., 2004), though it is uncertain how and why melting has changed. In particular, the region has strong natural climate variability, and this obscures any trends in the amount of warm Circumpolar Deep Water (CDW) present on the Amundsen Sea shelf (Dutrieux et al., 2014). The ungrounding of Pine Island and Thwaites glaciers suggest that ice loss from the Amundsen Sea sector may have started, or at least accelerated, in the 1940s (Clark et al., 2024; Smith et al., 2017), possibly triggered by a period of extreme natural climate variability (O'connor et al., 2023). However, events of the same magnitude are expected to have occurred several times over the last 10,000 years (O'connor et al., 2023), and the present retreat appears to be unprecedented during this period (Clark et al., 2024; Larter et al., 2014). The 1940s retreat is thought to have occurred prior to the onset of anthropogenically driven trends in forcings in the region (Holland et al., 2022). While ocean warming trends are thought to have occurred over the 20th century (Naughten et al., 2022; Naughten et al., 2023), they have only recently become statistically detectable, relative to the strong internal variability (Turner et al., 2025).

Several feedbacks have been identified that may be enhancing the retreat of Thwaites Glacier, implying that the changes may not be simply related to ocean forcing. These include increasing ice flux across the grounding line, due to a deepening bathymetry (Joughin et al., 2014) and the effect of the increasing ice damage on ice flow speed (Lhermitte et al., 2020; Surawy-Stepney et al., 2023). In addition, other feedbacks could be enhancing any increase in oceanic melt rates, such as changing ice shelf geometry and an increase in ocean melting area due to newly ungrounded ice (Arthern and Williams, 2017; Holland et al., 2023; Bett et al., 2024; De Rydt and Naughten, 2024).

It is essential to understand the historical drivers of and the processes that lead to Thwaites Glacier's thinning to understand and predict its contribution to future sea level rise. Therefore, in this study we explore possible quasi-steady pre-1940s Thwaites Glacier geometries, and the key processes responsible for its subsequent retreat. To do so, we employ a coupled ice/ocean coupled model, with additional idealised ice damage forcing and perform simulations over the 20th century. In a previous study (Bett et al., 2024) it was shown that simulating the future retreat of Thwaites Glacier required accurately resolving the ocean flow around pinning points which are crucial to the ice sheet evolution. It is not obvious that parametrizations of ice shelf melting will accurately represent these processes, suggesting that a coupled ice-ocean model should be used. These simulations retreat to and past the present-day grounding line, allowing us to isolate the effects of ocean forcing and idealised damage feedbacks on Thwaites Glacier's evolution. The paper proceeds as follows. In section 2 we analyse the 1947 imagery to provide new insight into the history of Thwaites. In section 3 we describe the coupled ice/ocean model used to examine the history of Thwaites, and the drivers of historical evolution. In section 4 we describe

https://doi.org/10.5194/egusphere-2026-669
Preprint. Discussion started: 2 March 2026

the use of this model to create example pre-1940s states and examine the processes and changes that occur as it retreats into the present-day configuration. In sections 5 and 6 we present our discussion and conclusions on the processes controlling the evolution of Thwaites Glacier.

2. Analysis of 1947 aerial imagery

Here we analyse aerial images of Thwaites Ice Shelf taken during the U.S. Navy operation Highjump in 1947 (USGS, 2018). To the best of our knowledge, this is the first time that these aerial images have been used to constrain Thwaites Ice Shelf geometry in detail in the pre-satellite era. Though the flight line and photo dataset locations themselves are approximate, we can identify key features like Mount Murphy and the Bear Peninsula, increasing the confidence of the provided locations. We examine images taken along two different flight lines, as shown in Figure 2 over the oldest cloud-free satellite image mosaic from 1973 (Miles and Bingham, 2024) for comparison.

Several key differences are observed in the comparison to the 1973 satellite image. In the 1947 imagery, we see western and eastern edges of a large ice tongue located at (a, b) and (e), with a large area of intact ice in between, as shown in (c, d). This suggests a pre-1940s western ice tongue that is much more advanced and less damaged than in the 1973 satellite imagery. The eastern edge shown in (e) is located in the middle of the main western ice shelf in the 1973 image, while the western edge shown in (a, b) is located in a region of icebergs and sea ice in the 1973 image, suggesting an eastwards shift in the outflow location between 1947 and 1973. We propose that these 1947 images are showing the large intact iceberg in the 1973 image before it detached from the ice shelf, with the ~64 km width of the iceberg (Figure 1a) matching the width of the 1947 photographed edges of the ice shelf (Figure 2). Additionally, the 1947 images show an intact ice shelf located at (h), where the shear margin is present in the 1973 image. Instead, the 1947 imagery shows a shear margin at the (f) and (g) locations further west, on a flow line passing through the western pinning point, suggesting a ~15 km eastward migration of the shear margin by 1973.

Despite uncertainty in image locations, these changes are large enough to suggest that Thwaites Ice Shelf underwent significant changes between the 1947 imagery and the oldest satellite image of 1973. In addition, the 1973 satellite image already strongly contrasts with the highly damaged present-day state. These early images were taken at a time (1947) that is close to the proposed timing of the ungrounding of the western pinning point (Clark et al., 2024), and so the ice shelf could already be in a period of change at the time of the imagery. We will use the evidence of the 1947 imagery and the 1973 satellite image, including the inference of an extended, less-damaged western ice shelf, to constrain our modelling of the 20th century evolution of Thwaites Glacier.

https://doi.org/10.5194/egusphere-2026-669
Preprint. Discussion started: 2 March 2026

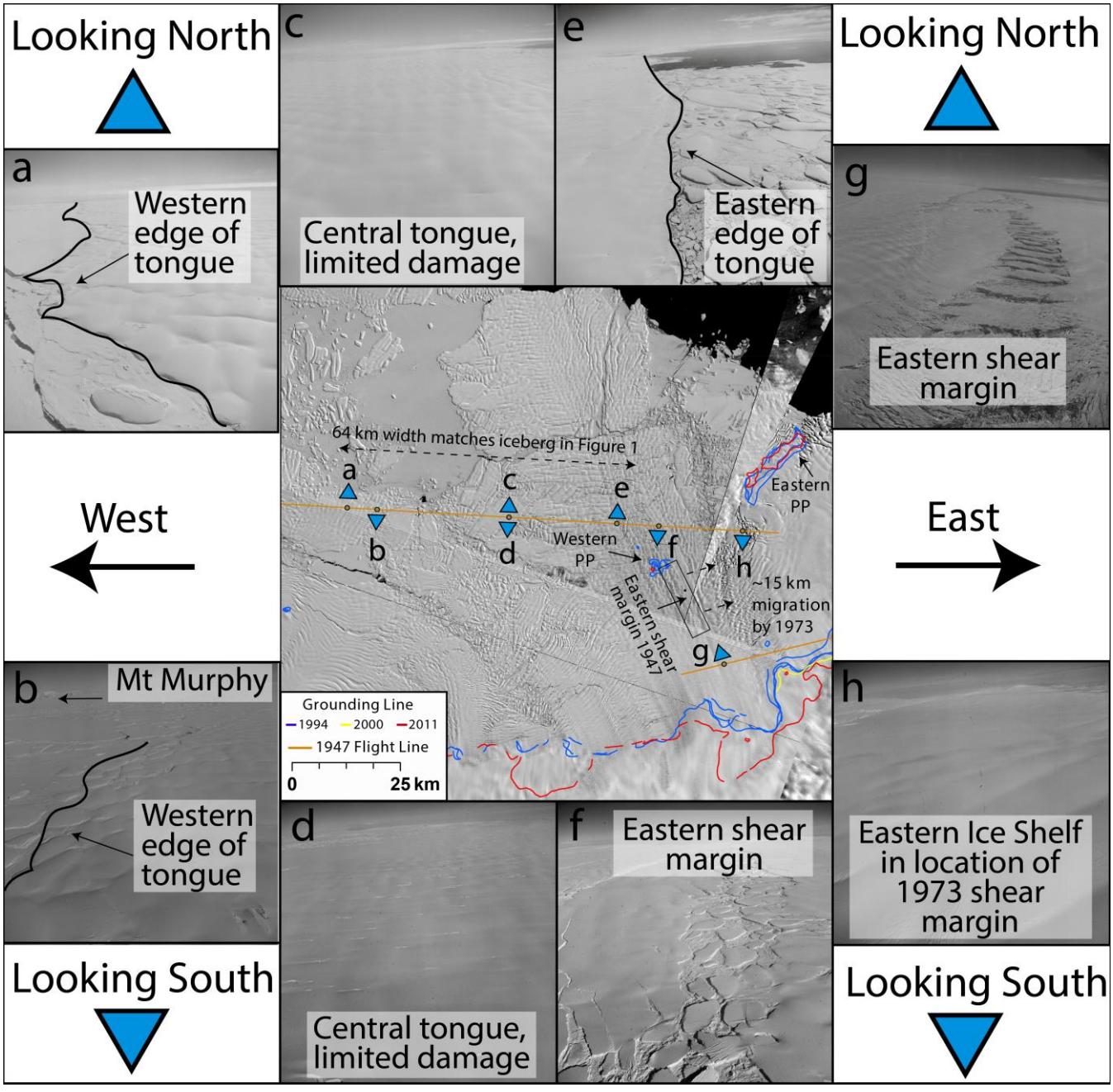

Figure 2: (centre) Geo-corrected Landsat-1 image mosaic from 1973 of Thwaites Ice Shelf (zoomed in compared to Figure 1a) (Miles and Bingham, 2024). Orange lines show two of the flight lines from the U.S. Navy operation Highjump in 1947 (USGS, 2018). (a-h) Snapshots taken along the flight paths at the indicated locations and directions in the central panel. Aerial photographs in panel (b,d,f and h), which were originally taken with a south-looking orientation from the place, have

https://doi.org/10.5194/egusphere-2026-669
Preprint. Discussion started: 2 March 2026

been horizontally mirrored to maintain a consistent orientation and facilitate direct visual alignment with panel (a,c,e,g) that were taken north-looking

3. Methods

3.1 Overview

We modify an existing coupled ice/ocean model setup (Bett et al., 2024) for the study of historical Thwaites Glacier evolution. First, we advance Thwaites Glacier from its present-day state to produce a pre-1940s example state. To do so, we use the large iceberg in the 1973 satellite image (Miles and Bingham, 2024) and the 1946/47 aerial imagery (USGS, 2018) as evidence to justify advancing the fixed ice front and healing the ice shelf damage, when starting from a present-day initialisation (approximately 2015). Next, we need to change the ocean forcing to reflect possible historical ocean forcings. Finally, we trigger retreat from this historical position, exploring the effects of both ocean forcing and introducing idealised ice damage. Each of these steps are explained in detail below.

3.2 Model structure

To capture complex ice/ocean feedbacks, such as those described above, we use the WAVI-MITgcm ice-ocean coupled model of the Amundsen Sea region, which is split into a coupled region and ice only domain (Figure 3a), as described in Bett et al. (2024). This coupled model uses a synchronous coupling procedure that splits the simulation into coupling periods, where the ice velocities are updated at the start of each coupling period, but then remain fixed during these periods, as the coupling period is also the timestep of the ice sheet model. However, the ice thickness updates continuously (i.e. during these periods), on the shorter ocean model timestep. No ice shelf melting is permitted on partially grounded ice sheet model cells, as in Bett et al. (2024) and as recommended by Seroussi and Morlighem (2018). Although the model includes the whole Amundsen Sea region including the PIG and Smith Glaciers, the modelling study focuses on Thwaites Glacier due to the strong contrast between the Thwaites Ice Shelf state in the 1947 aerial imagery discussed in this study and the present-day configuration and because the historical evolution of PIG has been considered in several previous studies e.g. (Reed et al., 2024; De Rydt et al., 2021; Bradley et al., 2025).

The WAVI ice sheet model is initialised to match the present-day Amundsen Sea glaciers, taking into account both the present-day surface elevation change signal (Smith et al., 2020) and the surface ice velocities (Mouginot et al., 2017a, b), as described by (Arthern et al., 2015; Bett et al., 2024). A Weertman basal drag coefficient field (C) is inferred under the present-day grounded ice extent during this initialisation, but outside of this area we apply a constant value $C=10^4$ Pa $m^{-1/3}$ $a^{1/3}$, as in Bett et al. (2024). The initially inverted model is then run forward in a relaxation step, which improves the surface elevation change match with observations, at the cost of a slightly worse match with ice speed and surface elevation (see Arthern et al. (2015) for full details). This starting state is similar to that used in Bett et al. (2024), but is using an updated

https://doi.org/10.5194/egusphere-2026-669
Preprint. Discussion started: 2 March 2026

temperature field generated using the BISICLES ice sheet model (Trevers et al., 2024). The bathymetry is based on Bedmachine V3 (Morlighem et al., 2020; Morlighem, 2022), but with the Pine Island Glacier cavity modified to match the field of Dutrieux et al. (2014).

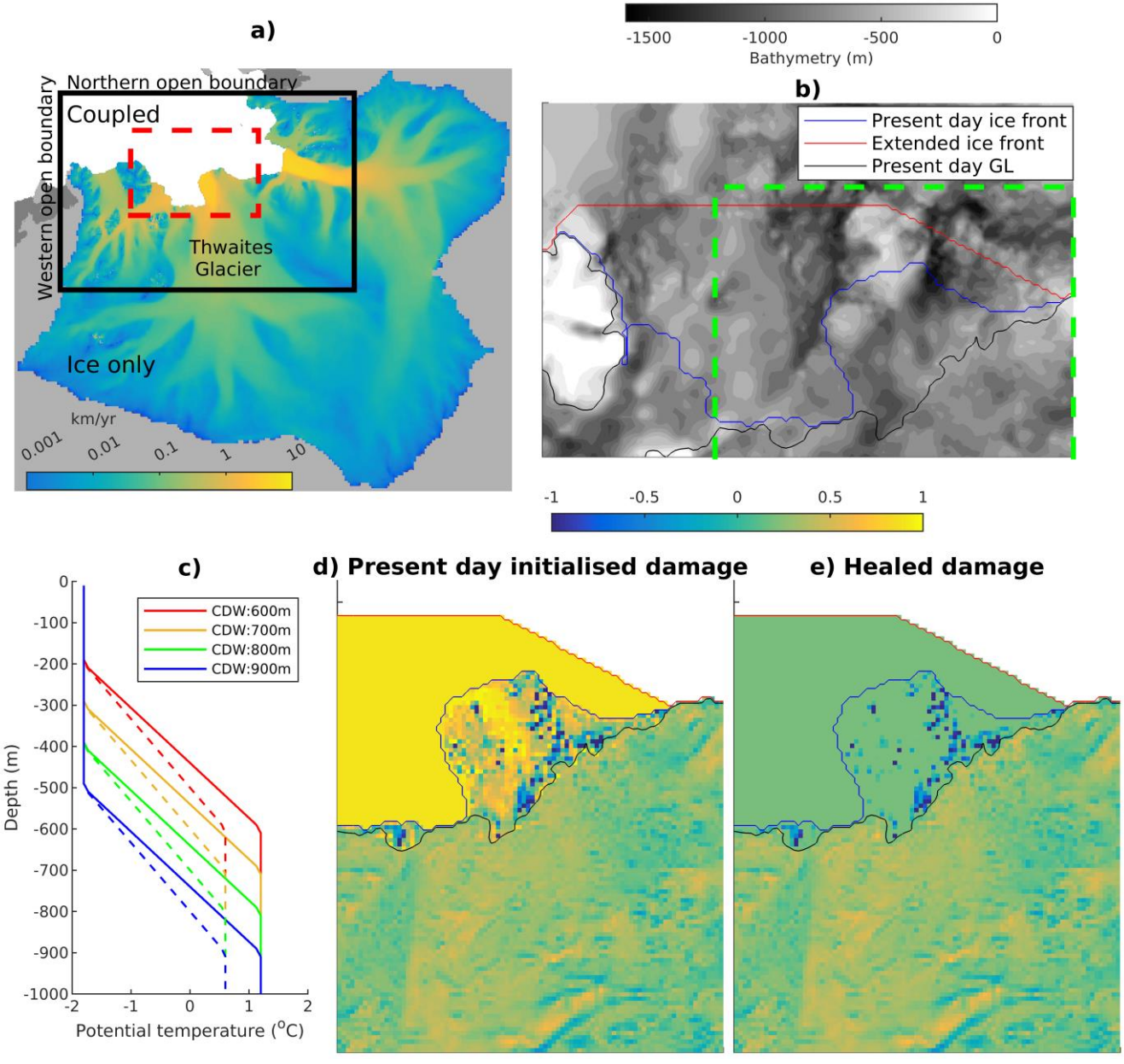

Figure 3: a) Amundsen Sea sector model domain, showing present-day model ice speed. The black rectangle shows the coupled model domain, and the remaining-coloured area shows the ice-only model domain. The red dashed box shows the

https://doi.org/10.5194/egusphere-2026-669
Preprint. Discussion started: 2 March 2026

area of panel b. b) Bathymetry (grey scale) for primarily the floating region of Thwaites Glacier, with present day ice front (blue), present day grounding line (black) and extended ice front (red). The green dashed box shows the northern, western and eastern bounds of the area plotted in later figures. c) Ocean temperature boundary conditions for the northern (solid line) and western (dashed line) coupled model domain boundaries, as in Bett et al. (2024). (d-e) Thwaites ice damage field saturated to range of 1 to -1 (as described in section 3.4), with present day ice front (blue) and grounding line (black) and extended ice front (red): d) Initialized, e) Healed.

In this study, we use three different types of simulations: 1) an ice-only with no ice shelf melting, 2) a reduced-physics (see below) coupled ice/ocean model, and 3) a full-physics coupled model. Models 1 and 2 are used only for the initial spin up of the initial historical starting states, while model 3 is used for all time-varying experiments. Model 2 (reduced-physics) is faster to run, with the aim of getting the ice state approximately adjusted, while model 3 (full-physics) is used for modelling accurate behaviour. The reduced-physics coupled model version has a spatially and temporally adaptive ocean lateral eddy viscosity, whereby the lateral eddy viscosity is increased when needed to ensure that the grid scale horizontal Reynolds number is less than 2 (Bryan et al., 1975). This has the advantage of avoiding the need for a short ocean model timestep, which allows us to perform much faster simulations to enable adjustment of the ice state, but will lead to high ocean eddy viscosity values where ocean velocities are relatively high, likely resulting in an underestimation of ice shelf melt rates. The reduced-physics coupled simulations use a longer coupling period and ice sheet model timestep of 80 days, along with a longer ocean model timestep of 800 seconds, compared to the 20 days and 100 seconds respectively used in the full-physics coupled model, with the same 20 days ice model timestep used in the ice only simulations.

3.3 Ice front

The ice model has the simplest possible representation of calving, with a fixed ice front. Thwaites present-day ice front, as used in the present-day model initialisation, is shown in Figure 3b and encompasses the full shear margin region between west and east Thwaites Ice Shelf. However, this ice front is greatly retreated compared to the ice front estimated from the 1947 imagery and the large iceberg in the 1973 satellite image. If fixed in the simulations, this retreated present-day ice front would limit where the model can ground and advance to. Therefore post-initialisation, for our historical Thwaites simulations we extend out the fixed ice front to an idealised pre-1940s historical extent, which is initially set to have ice thickness of 50 m. Using the evidence from the 1947 imagery and 1973 satellite image as a guide, an idealised extensive ice front is chosen (Figure 3b), removing restrictions that would have been placed by attempting to explicitly recreate the convoluted pre-1940s ice front and enabling the model to determine where the main outflows are within the area. The new idealised extended fixed ice front is set to join the three bathymetric highs that surround the area near Thwaites Ice Shelf (Figure 3b).

https://doi.org/10.5194/egusphere-2026-669
Preprint. Discussion started: 2 March 2026

3.4 Damage

During the ice model's initialisation into the present-day state, a 'viscosity enhancement' factor field (E) is recovered, which represents all spatial variations in viscosity that cannot be explained by the influence of temperature on strain-rate. In this study we assume that ice damage (D) is the primary source of viscosity enhancement, and we refer to D = 1-E as ice damage from now on. The damage field generated from the present-day initialisation is shown in Figure 3d for Thwaites Glacier and ice shelf. In this generated field there are high damage values in the western Thwaites Ice Shelf and particularly on the shear margin between eastern and western Thwaites Ice Shelf (Figure 3d), as might be expected (Figure 1b). Negative damage values represent areas where the ice model initialisation has increased the viscosity/strengthened the ice to match observations, relative to the viscosity expected from the ice temperature and strain rate. Outside of the present-day fixed ice front, where no values are generated by the initialisation, we apply a high damage value of 0.9, which effectively creates an ice front at the present-day location, because this highly damaged, relatively thin ice that has been added does not buttress the grounded ice.

During our evolving ice-ocean simulations we use this present-day damage field, plus a "healed" ice shelf damage field to represent the historical conditions seen in the 1946/47 aerial imagery and the iceberg on the 1973 satellite image, in which the ice shelf was much less damaged compared to the present day. To assign a damage value for the new "healed" field, the 1 decimal point rounded average damage on the initial present day grounded ice is calculated (0.2). This value is then applied as the maximum damage value past the present-day grounding line on the initially floating ice. The initially grounded ice damage values remain the same in this new field, but the initially floating ice is strengthened, as shown in Figure 3e.

Implementing a full time-varying physics-based damage model would clearly be preferable to this idealised approach, but that development represents a significant physical and technical challenge, that goes beyond the scope of the present study. Instead, the simulations attempt to capture potential ice shelf damage feedbacks in an idealised manner, using the two different damage fields. Our simple approach is that different damage values are applied depending on the spatial variability of the damage fields and depending on whether the ice cell is fully floating or not at the start of each ice/ocean coupling period. If the cell is grounded or partially grounded, then the value from the healed damaged field is used. If instead the cell is fully ungrounded, then damage is applied to that cell within the range of damages between the healed ice damage and the present damage field. The precise value within this range depends on a 'damage intensity factor' that we choose. If the damage intensity factor is 1 then the present-day damage value is applied to the fully ungrounded cell, if it is 0 then the healed damage value is applied. Essentially for damage intensity factor values above 0, when a cell becomes fully ungrounded during the evolving simulations, an idealised instant damage feedback is assumed to occur at that location. The

https://doi.org/10.5194/egusphere-2026-669
Preprint. Discussion started: 2 March 2026

damage intensity factor is an external parameter that we set in order to select a level of damage for the experiment we want to perform (see below).

3.5 Ocean forcing

The ocean boundary conditions on the western and northern boundaries for ocean velocities, temperature and salinity are applied similarly to Bett et al. (2024). However, in this study the Winter Water layer has been cooled down from -1 °C to -1.8 °C to better represent ocean conditions at the boundary location rather than warmer observations closer to the ice shelves, where warmer waters are upwelled (Dutrieux et al., 2014). We examine historical ocean changes by using deeper or shallower values for the thermocline depth in each simulation. The idealised profiles applied at the boundaries for temperature are shown in Figure 3c for varying thermocline depths which range from the warmest at 600 m to extreme cold conditions at 900 m depth, with 800 m to 600 m approximating the observed variability in the region between 1994 and 2012 (Dutrieux et al., 2014).

4. Results

In the following section, we first explore the changes required, when starting in a present-day configuration, to create an example reference quasi-steady pre-1940s Thwaites Glacier state, which is subsequently used as a starting point for more simulations. Next, we examine the key processes in a retreat that is triggered, firstly, using only enhanced ocean forcing (keeping the damage intensity factor set to 0), and, secondly, triggered using both enhanced ocean forcing and damage forcing (with damage intensity factor set to 1). By comparing these two retreats, we can decouple the roles of damage and ocean forcing in the 20th century retreat of Thwaites. Following this, further simulations are examined that branch off from a damaged retreating simulation, where the ice is allowed to subsequently heal. These simulations allow us to explore the role of feedbacks and determine whether there are other quasi-steady states within the Thwaites system with grounding lines advanced or similar to that of the present day position.

4.1 Spinning up to a reference pre-1940s quasi-steady Thwaites state

We start by considering the present-day configuration, with the modelled present-day ice flow shown as the red arrows in Figure 4a, showing the fast-flowing damaged western ice shelf (Bett et al., 2024). The corresponding melt rates are shown in Figure 4b, with high melt rates in the western Thwaites inlet (Figure 1) and low melt rates in the eastern Thwaites (Holland et al., 2023). To probe the processes responsible for Thwaites retreats into this present-day state, and beyond, we must first create an example pre-1940s Thwaites state as a starting point. Therefore, a quasi-steady example historical Thwaites

https://doi.org/10.5194/egusphere-2026-669
Preprint. Discussion started: 2 March 2026

geometry is spun up (Figure 4a), which will be referred to as the reference pre-1940s case. Using the intact ice shelf guided by the 1947 aerial imagery (USGS, 2018) and the intact iceberg in the 1973 image (Miles and Bingham, 2024) as our guide we use a damage intensity factor that is set to 0. Therefore, the healed damage field is used for both grounded and fully floating ice.

https://doi.org/10.5194/egusphere-2026-669
Preprint. Discussion started: 2 March 2026

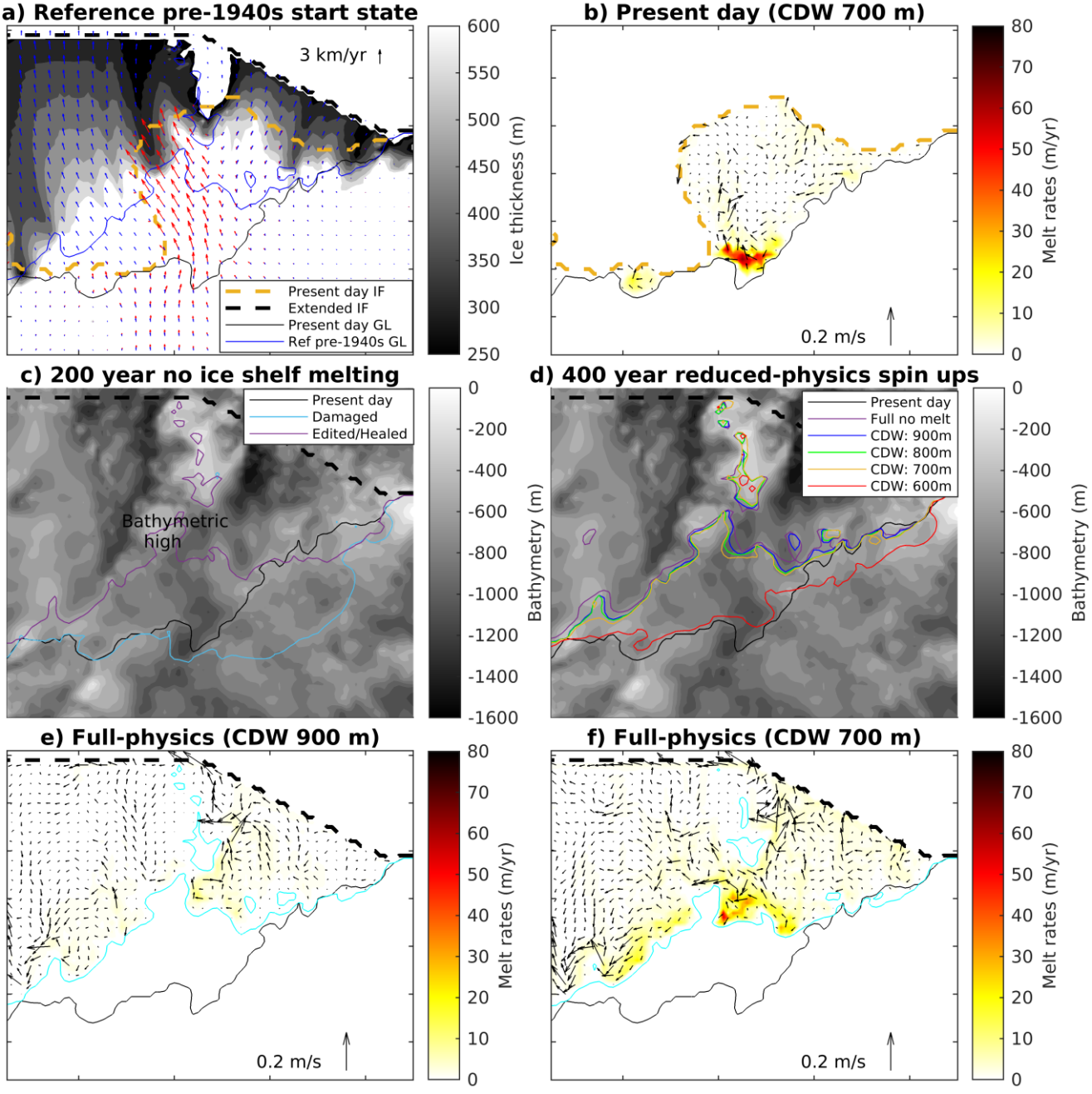

280

Figure 4: a) Ice thickness (saturated between 250 m and 600 m) and ice flow (blue arrows) and grounding line (blue contour) for the reference pre-1940s state. Present-day modelled ice flow (red arrows) and grounding line (black) are also shown. b) Ocean basal melting in present day state for 700 m thermocline depth forcing. c) Grounding lines after 200 years of ice-only simulation starting from present-day state, with healed ice shelf (purple) and with damaged ice shelf (cyan). d)

https://doi.org/10.5194/egusphere-2026-669
Preprint. Discussion started: 2 March 2026

Ice-only spin up grounding line after 2000 years (purple), and the subsequent reduced-physics-model grounding lines after 400 years for ocean forcings of 900 m (blue), 800 m (green), 700 m (orange) and 600 m (red). e-f) Basal melt rates for (e) 900 m forcing and (f) 700 m forcing after 200 and 300 years respectively of full physics coupled simulation starting from the chosen reference pre-1940s spun up state. Ocean boundary-layer velocities (black arrows) and grounding line (cyan) are shown. In all panels, present day grounding line position (black line), and extended ice front (dashed black) are shown, with the present-day ice front shown in a) and b) (dashed orange). Plotted over approximate area shown in Figure 3b by green dashed box.

The process to create this reference pre-1940s configuration involves several steps. First, we conduct the present-day initialisation described above and undertake the setup steps of extending the ice front and healing the ice shelf damage as described in section 3. Next, the ice-only model is run for 2000 years in total with zero ice shelf melting, following Reed et al. (2024). In the unedited ice geometry from the present-day initialisation there is retreat even with zero ice shelf melting, as found by Bett et al. (2024) and Williams et al. (2026), but after extending and healing the ice shelf the grounding line advances (comparing at a partial spin up time of after 200 years in Figure 4c). In this edited setup, the ice first regrounds on the western pinning point, and then the main grounding line advances from the present-day position to encompass the western bathymetric high (Figure 4c). Healing of the ice shelf damage and the extension of the ice front are essential to enable this grounding line advance, suggesting that the present-day ice loss is strongly controlled by ice front retreat and the ice damage feedback: the only way to reverse the ice loss is to heal the damage and advance the ice front.

After a quasi-steady state is achieved with zero melting after the full spin up of 2000 years (Figure 4d), the reduced-physics coupled model is run for 400 years to adjust the state approximately to the presence of ocean forcing. This step is repeated for each of the different CDW thicknesses applied at the boundaries (Figure 4d). For the three colder ocean forcing conditions (thermocline depths of 900 m, 800 m and 700 m), Thwaites grounding line remains quasi-steady and still advanced to the western bathymetric high after 400 years of reduced-physics coupled spin-up (Figure 4d). However, the warmest case (600 m thermocline) retreats off the bathymetric high, as labelled in Figure 4c, during the spin up simulation, back to the present-day grounding line, and is still retreating at the end of the simulation (Figure 4d).

For the simulations that remain on the bathymetric high, a key feature of the configuration is that the grounding line is advanced compared to the present day, such that there are the two separate wide and slow outflows, with a western outflow and an eastern outflow (blue arrows in Figure 4a). The western outflow creates an ice tongue comparable to the 1947 photographs (Figure 2) and 1973 iceberg (Figure 1a) and is in stark contrast to the heavily damaged present-day western ice shelf. The eastern outflow feeds ice eastwards through what is currently the Thwaites Eastern Ice Shelf. The western grounding line sits on the bathymetric high, while the east still has a pathway at depth for warm CDW to access the eastern grounding line (Figure 4d).

https://doi.org/10.5194/egusphere-2026-669
Preprint. Discussion started: 2 March 2026

In all of the full-physics coupled model simulations that follow, we start from the reference pre-1940s case that has an advanced ice front, fully healed damage, and had the reduced-physics coupled model spin up with 900 m CDW thermocline depth. This is the state shown in Figure 4a, with the grounding line also shown in blue in Figure 4d.

4.2 Retreating Thwaites simulations with ocean melting and ice damage

We first re-test the non-retreating cases that occurred during the reduced-physics spin ups with the full-physics coupled model. We now start simulations from the reference pre-1940s spun up state, and use fully healed damage (damage intensity set to 0) and ocean forcings ranging from 900 m to 700 m thermocline depth. Similar to the reduced-physics spin-ups, Thwaites Glacier remains grounded on this bathymetric high for these ocean forcings. After 200 years of full-physics 900 m thermocline simulation there is no noticeable grounding line change from the reference pre-1940s spun up state, which used the same ocean boundary forcing (Figure 4a,e). Similar to the reduced-physics simulation, the full-physics simulation with 700 m thermocline also stays on the bathymetric high after 300 years, despite its higher melt rates (Figure 4f). For both cases the melt rates are highest in the eastern outflow (Figure 4e,f).

To examine the key processes that occur during retreating Thwaites Glacier simulations, we use the full-physics coupled model and trigger retreat under a range of different thermocline depths and levels of floating ice damage. Initially we examine two warm ocean forced cases with the base of the thermocline depth at 600 m: One with an intact ice shelf, with damage intensity set to 0, and a second case with a damaged ice shelf, with damage intensity factor set to 1. These will be referred to as the 'ocean only forced' and the 'ocean plus damage forced' simulations. In both cases the ocean boundary forcing is instantaneously changed, and the ice damage ramps up over 5 years, from the reference pre-1940s simulation, and we observe the subsequent evolution. We first consider the ocean forced only simulation.

4.2.1 Retreating Thwaites Glacier with ocean melting only

One of the key processes during Thwaites retreat is the ungrounding of the western pinning point, which we examine initially using the ocean only forced simulation. In this simulation it takes a long time for an ocean passage to open up upstream of the western pinning point (~365 years, Figure 5c,d), with this timing most likely being made longer due to not allowing melting on partially grounded cells in these simulations. However, as soon as this passageway opens up, a redirection of the main melt-water flow happens, with an east-to-west flow through this new ocean passageway enhancing high melt rates south of the western pinning point (Figure 5a,c). The resultant thinning of ice upstream of the bedrock high causes an ungrounding of the pinning point (Figure 5e,f), leading to increased ice velocities in western Thwaites and grounded ice thinning (Figure 5e,f), similar to the modelled effect of future Thwaites pinning point ungroundings (Bett et al.,

https://doi.org/10.5194/egusphere-2026-669
Preprint. Discussion started: 2 March 2026

2024). This subsequent ice speed up and thinning occurs with rapid western grounding line retreat to near present-day grounding line position, with high melting in western Thwaites similar to the present day (e.g. Holland et al., 2023; Nakayama et al., 2019)) . We also observe separate slow retreat in eastern Thwaites.

355

https://doi.org/10.5194/egusphere-2026-669
Preprint. Discussion started: 2 March 2026

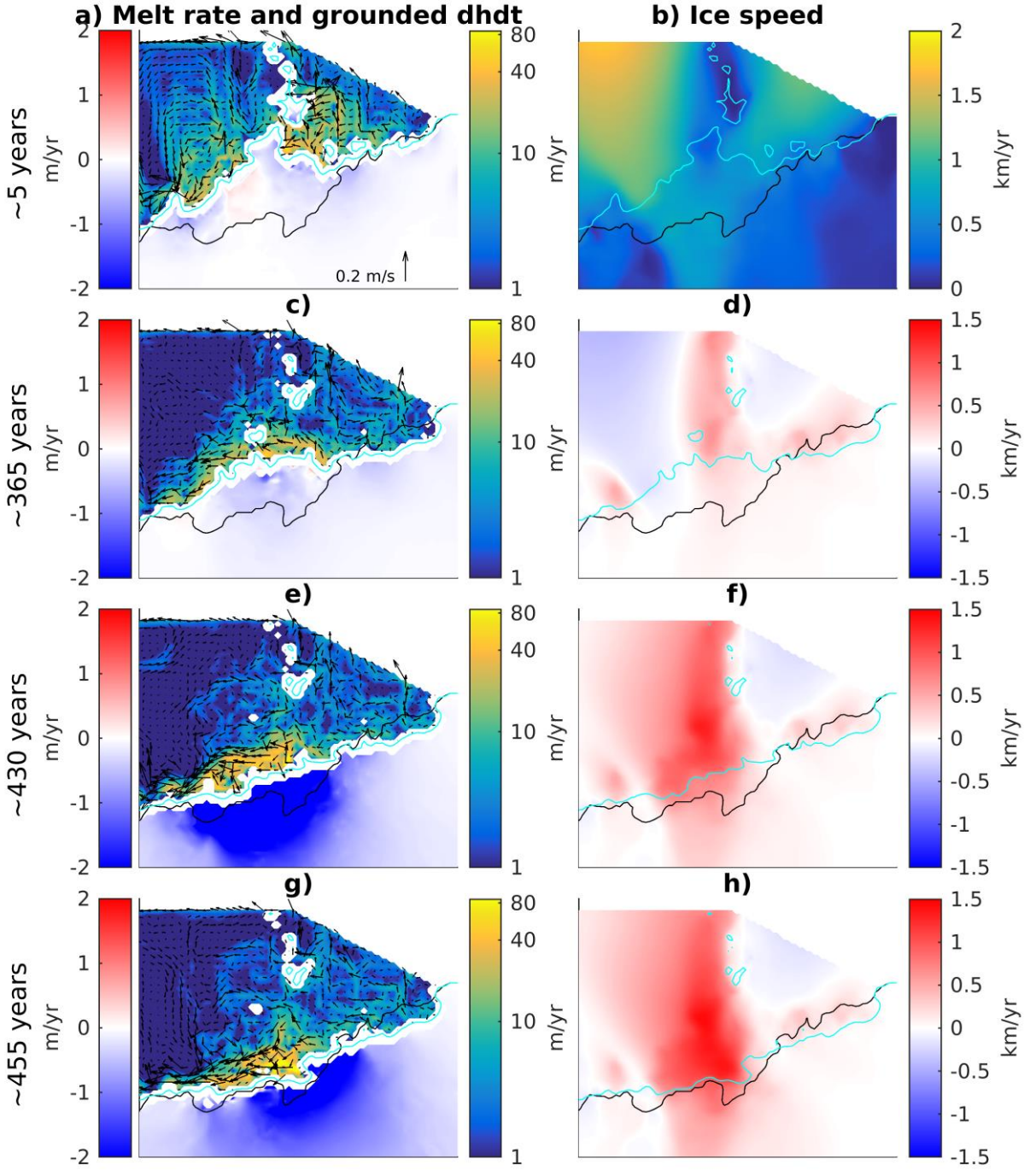

Figure 5: Snapshots taken during the ocean only forced simulation: (a,c,e,g) ice shelf melt rates with ocean boundary-layer velocity vectors (on fully floating ice only) and ice thinning rates (on fully grounded ice only). (d, f , h) Ice speed changes

https://doi.org/10.5194/egusphere-2026-669
Preprint. Discussion started: 2 March 2026

relative to those shown in b). For each plot the snap-shot grounding line (cyan) and the present-day grounding line (black) are shown. Plotted over approximate area shown in Figure 3b by green dashed box.

4.2.2 Effect of ice damage and future retreat

As discussed above, comparing the intact 1947 Thwaites western ice shelf and intact iceberg in the 1973 satellite image, with the already damaged state of western Thwaites in the 1973 image and the heavily damaged present-day western Thwaites, it is apparent that damage has played an important role in the evolution of Thwaites Ice Shelf. During the damage plus ocean forced simulation, faster grounding-line retreat occurs to the observed 1996 grounding line (~85 years) compared to the ocean only forced case (~455 years), primarily because the western ocean passageway is opened without delay (Figure 6a,b). In the ocean plus damage forced simulation, this retreat recreates the present-day ice shelf configuration, with a highly damaged fast-flowing western Thwaites Ice Shelf (Figure 6d), in contrast with the slower, broader outflow in the ocean only forced case (Figure 6c).

https://doi.org/10.5194/egusphere-2026-669
Preprint. Discussion started: 2 March 2026

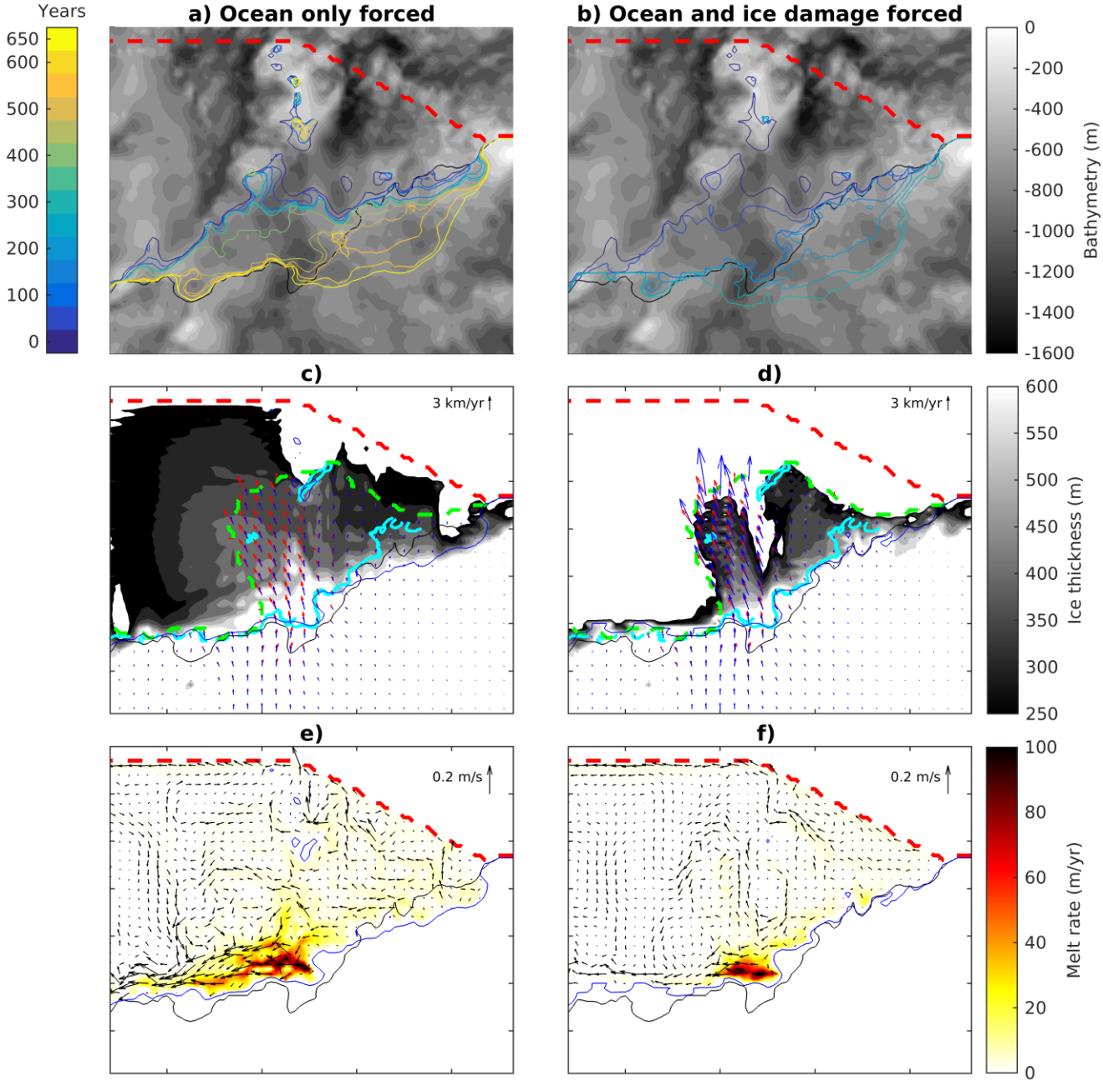

Figure 6: (a and b) Grounding line snapshots at 50-year intervals during (a) the ocean only forced simulation (650 years) and (b) ocean plus damage forced simulation (300 years). (c and d) Ice thickness and velocities after retreat to approximate best match 1996 grounding line (cyan; (Rignot et al., 2016)) for (c) ocean only forced retreat (shown at ~455 years) and (d) ocean plus damage forced retreat (shown at ~85 years), where ice thickness is plotted between 250m and 600m only.

https://doi.org/10.5194/egusphere-2026-669
Preprint. Discussion started: 2 March 2026

Velocities are plotted over only the present-day ice shelf area for both the present-day model (red) and the simulation in question (blue). (e-f) Ice shelf basal melt rates for the same snapshots with ocean boundary-layer velocities (black arrows) and grounding line (blue). In all plots present day grounding line position (black line), and extended ice front (dashed red) are shown, with the present-day ice front also shown in c) and d) (dashed green). Plotted over approximate area shown in Figure 3b by green dashed box.

In the ocean only forced case, the initial pinning point ungrounds fully and then the western retreat occurs, after which the western pinning point regrounds for a while, as the thick upstream ice drains. However, in the ocean plus damage forced case the pinning point only fully ungrounds after the western retreat and doesn't reground as the upstream ice drains, due to the strain-thinned damaged western ice shelf. After this initial rapid retreat, both cases have grounding lines that pause around the real 1996 grounding line position (Figures 6c and 6d), although there is a difference in the spatial pattern of the retreat, with the ocean only forced case retreating eastern Thwaites beyond the 1996 grounding line, by the time the western retreat has occured. This is because the ocean only forced case takes a long time to unground the western pinning point and during this time a slow eastern retreat occurs. After the initial western retreat, both simulations have a large retreat that is focussed on eastern Thwaites, while also retreating in the west to the initial 2015 model grounding line and beyond, but with more western retreat occuring in the ocean plus damage simulation.

4.2.3 Ice piracy of Eastern Thwaites

The large grounding line retreat in eastern Thwaites (Figure 6a,b), after passing through the present-day grounding line, is a common feature of model projections in this sector (Nias et al., 2019; De Rydt and Naughten, 2024; Bett et al., 2024). Ice shelf damage (Figure 3d) and melting (Figure 4b, Figure 6e,f) are both lower in eastern Thwaites compared to the west. However, both are still playing some role in this retreat: from the start of the simulations, before any western retreat, a separate very slow eastern retreat occurs in both the ocean forced only and ocean plus damage forced simulations, as the simulation adjusts to changes in ocean and damage forcing (Figure 6a, b). The rate of eastern ice retreat sees a large increase after the grounding line completes the historical retreat in the west, to its 1996 position (Figure 6 a,b), which occurs much earlier in the ocean plus damage forced simulation. This suggests a possible east—west coupling may be driving the eastern Thwaites retreat.

With the ungrounding of the western pinning point we see a rerouting of ice flow on the ice shelf. When the grounding line is advanced in the pre-1940 reference state, ice flow is diverted into eastern Thwaites Ice Shelf, but when it is ungrounded and the grounding line retreats, this opens a new pathway for ice flow directly over the former western pinning point's position (Figure 4a). This is shown more clearly by considering a boundary defined by the streamline that flows through the eastern edge of the present-day eastern pinning point location (Figure 7a,b). This streamline shifts eastward as the

https://doi.org/10.5194/egusphere-2026-669
Preprint. Discussion started: 2 March 2026

simulation's western grounding line retreats, and crucially moves past the current western outflow and Thwaites Inlet locations (Figure 1), as shown in Figures 7a,b. Therefore before the retreat, Thwaites Inlet flows out through the eastern ice shelf, but after retreat it now flows out through the western outflow (Figure 7a,b). This diversion starves the flow of ice to the eastern ice shelf, leading to thinning through 'ice piracy' (e.g. Selley et al., 2025; Mccormack et al., 2023; Conway et al., 2002). Comparing the flow of the western ice shelf before and after the retreat to the 1990s position also indicates ice acceleration and a westward shift, away from the eastern pinning point (Figure 7a,b), reducing the flow of ice that interacts with this pinning point. This change is enhanced in the damaged simulations, due to the decoupling of western and eastern Thwaites Ice Shelf by the increased western damage (Figure 6c, 6d).

https://doi.org/10.5194/egusphere-2026-669
Preprint. Discussion started: 2 March 2026

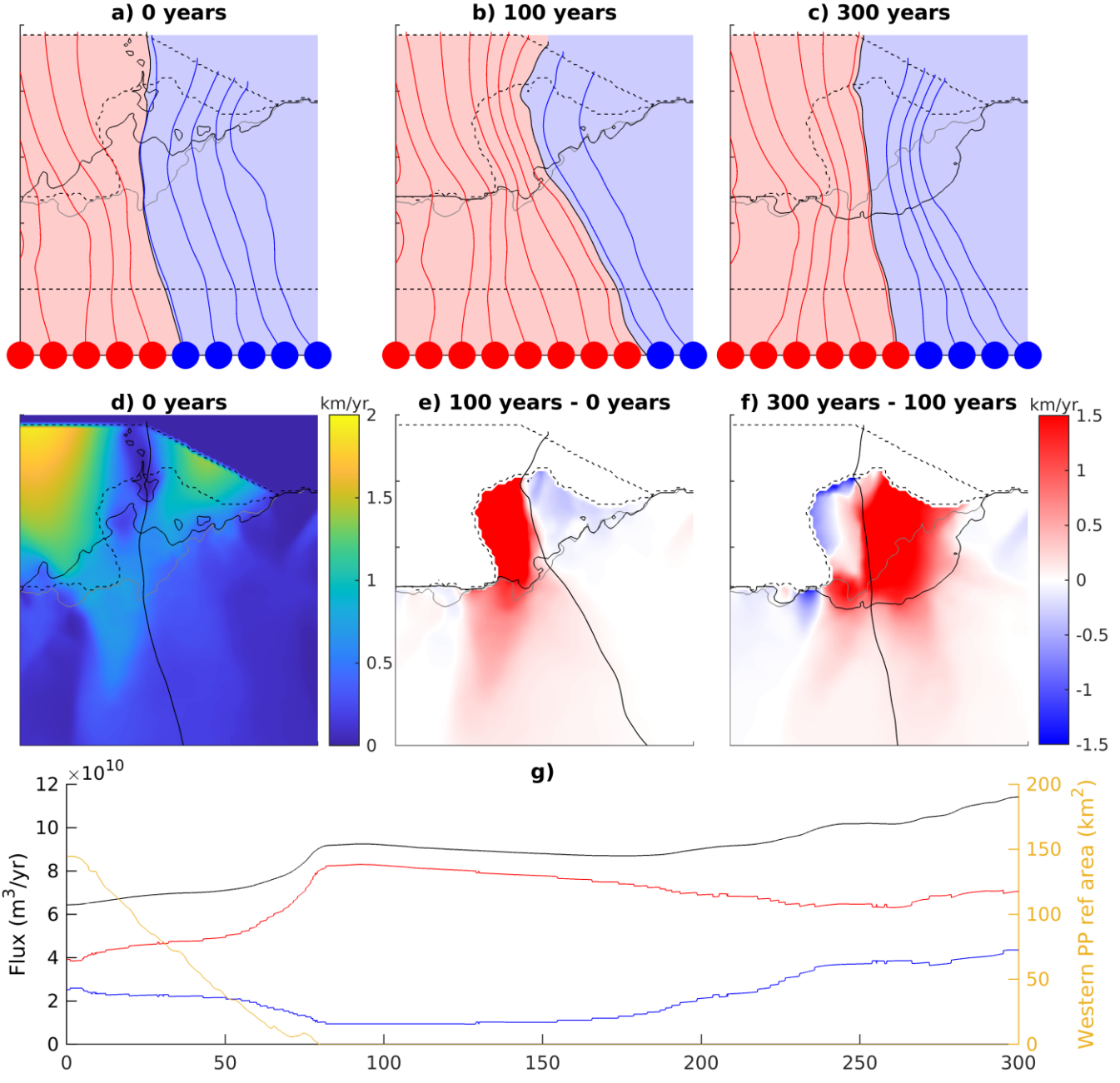

Figure 7: Ocean plus damage forced simulation. (a-c) Snapshots of grounding line position (east-west black line) and streamlines of ice flow, with red denoting area drained by western Thwaites Ice Shelf and blue drained by the eastern Thwaites Ice Shelf for: a) 0 years, b) 100 years and c) 300 years. The east/west boundary (north-south black streamline) is defined by the streamline passing through the eastern edge of the present-day eastern pinning point location. The present-day

https://doi.org/10.5194/egusphere-2026-669
Preprint. Discussion started: 2 March 2026

grounding line is shown by a grey line. (d) Ice speed at 0 years (pre-1940s reference state) and (e-f) differences between selected snapshots over the present-day ice extent. g) Timeseries of ice flux through the straight black dashed line through Thwaites basin shown in (a-c) separated into total (black) as well as west (red) and east (blue) using the boundary line between west and east outflow. Total grounded area on western pinning point is shown in orange. Plotted over approximate area shown in Figure 3b by green dashed box.

The change in buttressing from the western grounding line retreat also leads to ice piracy upstream on the grounded ice, with the boundary between the outflows shifting so that more of the catchment drains out via the newly created Thwaites Inlet (Figure 1, 7b). In addition, an acceleration occurs in the west, while a deceleration occurs in the east (Figure 7e). We see an overall increase in ice flux after the retreat, agreeing with satellite observations (Mouginot et al., 2014), and an increase in the flux through the western grounding line, but crucially a reduction in ice flux through the eastern grounding line at the same time (Figure 7g). This flux change is due both to the changes in the ice speed and change in the position of the boundary between the outflows. This historical ice piracy then starves eastern Thwaites grounded glacier, leading to the present day/future retreat in eastern Thwaites (Figure 7c,f), despite eastern Thwaites grounding line lying on top of a high bathymetric ridge (Figure 6a,b). After 300 years, eastern Thwaites has completely ungrounded from the ridge, retreated quickly through a deeper basin to the next bathymetry ridge (Figure 6a,b) and all newly formed eastern pinning points have ungrounded (Bett et al., 2024). This causes the flux to increase in the east again (Figure 7g), due to ice speed up and a shift in the east/west boundary (Figure 7c, f) and we see a strong reduction in eastern retreat rates (Figure 6a,b). Thus, the ice piracy is a transient phenomenon that seems to be centred on the present day.

4.3 Multiple quasi-steady states

We now have a good understanding of the processes occurring during the retreat of Thwaites from our reference pre-1940s state. Next, we want to understand the controls on this retreat: is it directly maintained by ice shelf melting, or are ice and ocean feedbacks playing an important role? This question is related to whether there are other quasi-steady states in the system, intermediate between the advanced reference pre-1940s state we have been considering, and the present-day retreating ice geometry. Furthermore, this investigation has an important practical implication: if there are any other quasi-steady states, they may also be possible options for a historical pre-1940s Thwaites Glacier configuration. To probe the existence of other steady states, we conduct a suite of reversibility experiments, in which we vary ice damage and ocean forcing through time.

Our methodology is illustrated in Figure 8a, which shows the evolution of grounded ice area under different ocean forcing thermocline heights (line colour) and imposed ice damage states (line style). The ocean only forced and ocean plus damage forced simulations are visible in this plot as the red solid and red dashed lines, respectively, that start from time zero, illustrating the retreat that occurs in both cases. The methodology is as follows: to search for new quasi-steady historical

https://doi.org/10.5194/egusphere-2026-669
Preprint. Discussion started: 2 March 2026

configurations, we start with a damaged forced simulation (damage intensity factor set to 1), but to potentially aid in finding new quasi-steady states, a slightly cooler and less extreme ocean forcing, equivalent to present day (700 m thermocline height) is applied. This simulation is shown as the orange dashed line in Figure 8a and also retreats in a similar way to the ocean plus damage simulation shown above. Sets of simulations are then branched off from this retreating simulation, after selected events: after the ocean passageway has opened upstream of the western pinning point (80 years), and after grounding line retreat to near the 1990s position (110 years), as shown in Figure 8a. Crucially, the healed damage field is re-applied to these simulations (damage intensity factor set to 0), so they re-form an intact ice shelf again. The branching sets are simulated for several centuries and are forced with a range of ocean forcings, with thermocline depths between 900m-600m, such that 4 coloured lines emerge from each branching point (but all solid lines – healed ice). Additionally, the initial simulations are shown from our initial pre-1940s reference state, both for damaged and healed ice.

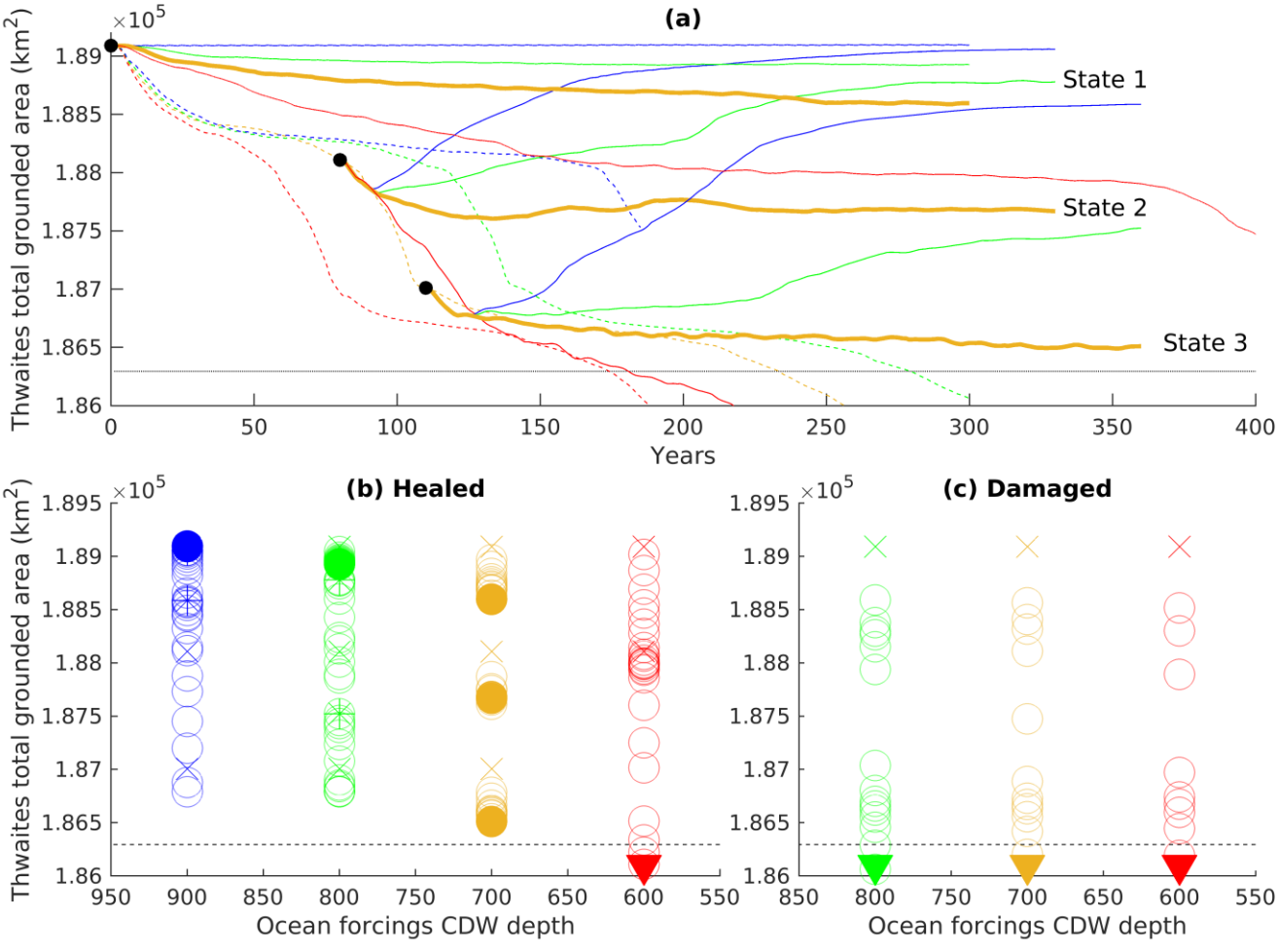

Figure 8: a) Total grounded area, over Thwaites basin, with line colour representing ocean forcing thermocline height and line style representing damage (Ocean forcing: blue = 900 m, green = 800 m, orange = 700 m and red = 600 m. Damage:

https://doi.org/10.5194/egusphere-2026-669
Preprint. Discussion started: 2 March 2026

dashed = present-day damage, solid = healed damage). Branch off times at 80 and 110 years marked with black circles for chosen simulation. The horizontal dashed black line indicates the present-day grounded ice extent. b) Scatter of grounded area against ocean forcing applied, where the cross demotes the starting point for a simulation, open circles are plotted every 20 years, and a solid circle indicates a quasi-steady state; a solid arrow indicates no steady state was found. c) Same as b) but for damaged simulations.

All simulations starting from the reference pre-1940s state with ice damage retreat past the present-day grounding line extent (dashed lines in Figure 8a). In contrast, only the warmest (600 m thermocline forcing) undamaged state retreats past the present-day grounded area extent (solid lines starting from 0 years, with red line case shown in Figure 6a). For cooler undamaged simulations, the ice remains in a quasi-steady state. For future reference, we refer to the quasi-steady state in the reference pre-1940s state, and maintained by the undamaged simulations, as 'state 1' (Figure 8a). This is the state we have been discussing so far, with the ice fully grounded all the way out to and including the western pinning point.

We next consider the cooler 700m damaged case (orange dashed line) and branch a set of damage-healed simulations after the passageway has opened up behind the western pinning point (80 years). As expected from our earlier warm ocean forced only simulation, the branched simulation with the warmest 600 m forcing rapidly retreats, even though the ice is healed, as the ocean passageway is already open and the western pinning point exposed for rapid ungrounding through melting upstream. With the two coldest ocean forcings (CDW thickness of 900m and 800m) the grounding line re-advances onto the western bathymetric high and returns into state 1 (Figure 8a). However, for 700 m thermocline height, we find that the ice attains a new quasi-steady state, which we refer to as state 2. In state 2, the ice sheet is able to sustain an open channel behind the western pinning point without retreating.

If we continue along the retreating damaged 700m thermocline case, we get similar results for the set of simulations branched after 110 years, in a state close to the 1990s grounding line. Again, we see that the two coldest cases re-advance to produce earlier states and both appear to trend to state 1, while the 700 m thermocline healed case obtains a new quasi-steady state, state 3. Thus, when starting from our three different starting points, we find three distinct quasi-steady states for Thwaites Glacier. This has the important implication that ice loss from Thwaites Glacier is not always simply-forced or reversible. States 1-3 all have the same ice damage state (healed) and ocean forcing (700 m thermocline), but are 3 independent quasi-steady states, any of which could have been applicable for the pre-1940s period.

In this analysis, we avoid labelling the states as 'steady', favouring instead 'quasi-steady' because the ice volume above floatation is still adjusting to the new grounding lines at the end of the 250-year simulations. Indeed, it is also clear from the ocean only forced simulation that retreats can occur many centuries after an overall grounded area appears steady (Figure 8a, red solid line), as in this case a slow ungrounding upstream of the key western pinning point occurs before 365 years (Figure

https://doi.org/10.5194/egusphere-2026-669
Preprint. Discussion started: 2 March 2026

5, 6a), which is not clearly captured with an overall grounded area metric. With this coupled modelling system, which is necessary to study pinning-point ungrounding, computational expense prohibits us from running these simulations for longer. Therefore, it's possible that these quasi-steady states may still retreat if simulated for long enough. However, the centennial time scale studied here is the period over which retreat and steady states are of interest to policy questions around sea-level rise and greenhouse-gas emissions.

In summary, with a healed ice shelf these simulations suggest a quasi-steady stability landscape where cooler thermocline depths of 900 m and 800 m have one quasi-steady grounding line at the fully advanced state 1, then intermediate present-day 700 m forcing has three quasi-steady grounding lines (states 1-3), and finally the warmest 600 m thermocline height leads to no steady grounding lines within the area we are considering (Figure 8b). Crucially, however, when the ice shelf is damaged none of these quasi-steady grounding lines exist for the tested forcings between the observed ocean range of 800 m-600 m thermocline height (Figure 8c). Additionally, the even colder 900 m thermocline height case appears to be retreating as well after 185 years (Figure 8a), before the model becomes numerically unstable for the applied model timesteps, due to the unphysical combination of high ice shelf damage and very low ice shelf melting during the modelled rapid retreat.

Therefore, we have found three distinct quasi-steady coupled ice/ocean states for Thwaites Glacier (Figure 9). State 1 is the state described previously and used as the starting point in the retreating simulations, with grounding line fully advanced onto the western bathymetric high (Figure 9a). State 2 has an open channel upstream of the western pinning point but is still advanced compared to 1990s/2015 observed grounding lines (Figure 9c). State 3 also has open water upstream, but has a much larger cavity as the grounding line is in a similar position to the observed 1990s position (Figure 9e). In all states the western pinning-point is grounded, but the extent of the grounding varies. Between the states 1 and 2/3 we see a change in ocean currents as the ocean channel opens upstream of the western pinning point (Figure 9 b,d,f), as described previously (Figure 5). This change shifts the highest melt rates from the eastern Thwaites to upstream of the western pinning point as the state progresses from state 1 (Figure 9b) to state 2 (Figure 9d) and then finally to state 3 (Figure 9f). The further grounding line retreat in state 3 leads to more concentrated melt rates upstream of the western pinning point, with the highest melt rates occurring in this state due to the deeper grounding line in this location. This represents a positive melting feedback onto the ice retreat. We re-emphasise, however, that all of these states only exist for undamaged ice. With present-day ice damage, we do not find any quasi-steady states for Thwaites Glacier.

https://doi.org/10.5194/egusphere-2026-669
Preprint. Discussion started: 2 March 2026

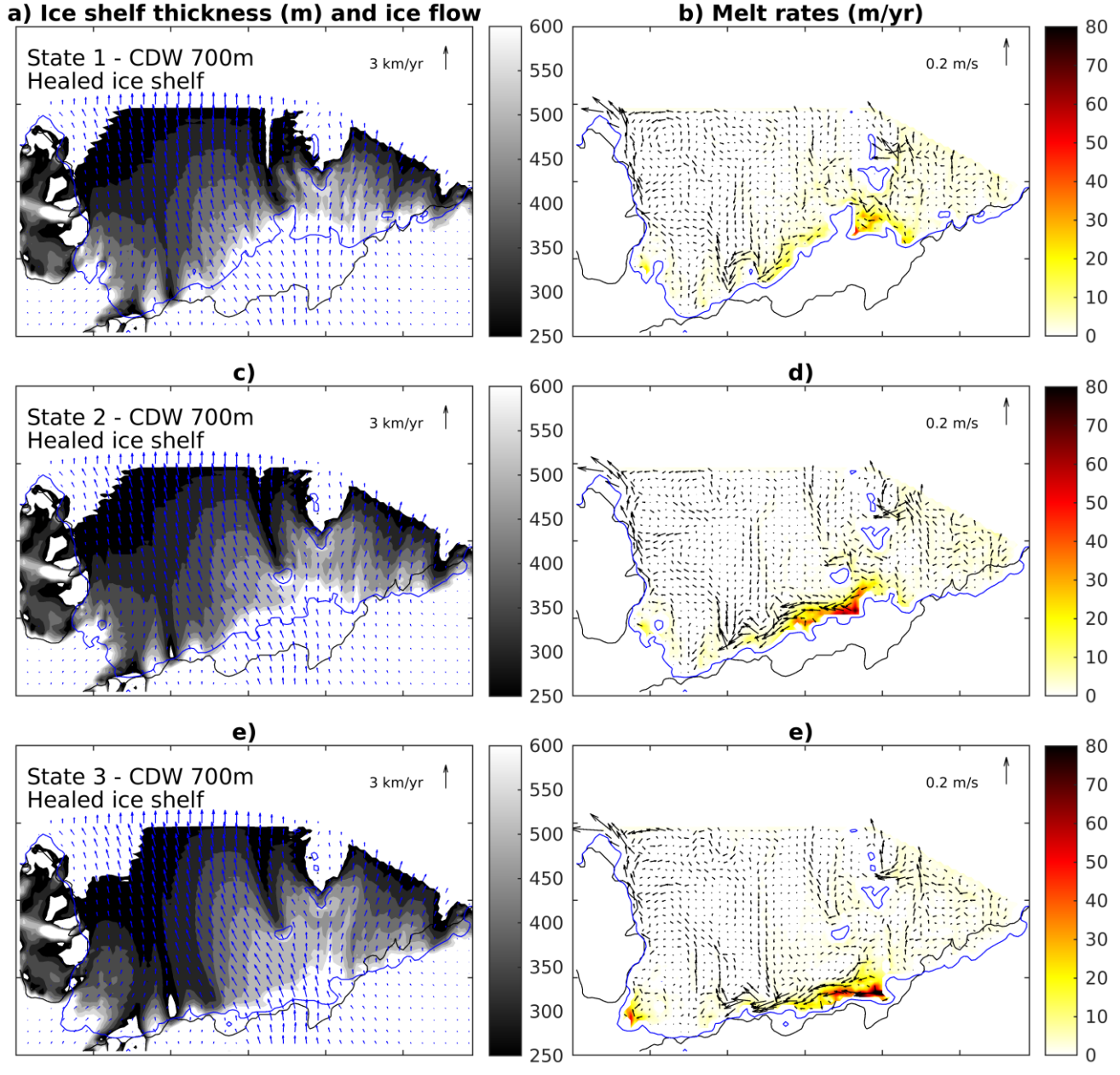

Figure 9: Ice velocities (blue arrows) and ice thickness saturated between 250m and 600m for: a) state 1, c) state 2, e) state 3. Ocean boundary-layer velocities (black arrows) and ice shelf melt rates (colour) for: b) state 1, d) state 2, f) state 3. Present day grounding line (black contour) and chosen state grounding line (blue contour). Plotted over approximate area shown in Figure 3a by red dashed box.

https://doi.org/10.5194/egusphere-2026-669
Preprint. Discussion started: 2 March 2026

5. Discussion

This study considers the evolution and drivers of the retreat of Thwaites Glacier over the 20th century. In this paper, we have analysed 1947 aerial imagery over Thwaites Ice Shelf, which suggests a western shift in the western ice shelf and the shear margin, compared to the present day. We have shown that healing and extending the ice shelf is required to create a quasi-steady reference pre-1940s Thwaites Glacier. In simulations retreating from this example state, we have highlighted several key processes, including the ungrounding of the western pinning point, and the effects of ice damage. Additionally, we have highlighted a new process for Thwaites Glacier, the transient effect of ice piracy between western and eastern Thwaites, which could help explain the observed present day eastern Thwaites grounding line retreat. Furthermore, we found that with a healed ice shelf multiple quasi-steady grounding line positions exist for the same ocean forcing, implying that Thwaites Glacier's historical retreat may have a complex, non-linear response to ocean warming. However, Thwaites Glacier retreats through all these grounding-line positions when present-day ice shelf damage is applied, for all simulated ocean forcings, implying the importance of damage feedbacks on the stability of Thwaites Glacier. In this section, we discuss the implications of these results and contextualise them amongst the current literature of past and future Thwaites retreat.

5.1 Western pinning point ungrounding and retreat

To obtain a reference pre-1940s state, the present-day Thwaites configuration is edited by healing damage and extending the ice front. Once a historical state was found, simulations were set off from this state with varying degrees of damage and ocean forcing applied. In these simulations we model the process of melt-driven ungrounding of the historic western pinning point of Thwaites Ice shelf. Western pinning-point ungrounding triggers rapid grounding-line retreat to near the present-day position. In these simulations, retreat occurs with warm ocean forcing, using a 600m thermocline depth, which is the equivalent of the warmest observed conditions in the region (Dutrieux et al., 2014). However, this threshold is highly uncertain and will depend on the modelling choices made in this study, for example due to parameter uncertainty in areas such as ice rheology and basal sliding. In particular, the ocean only forced simulation takes a long time (~365 yrs) to open the ocean passageway upstream of the western pinning point. This may suggest that we are too conservative with ice shelf melting near the grounding line, where no ice shelf melting is applied on partially or fully grounded model cells. Furthermore, we may be missing complex grounding line processes (Rignot et al., 2024; Bradley and Hewitt, 2024), which may speed up the initial opening up of the ocean passageway, with another study finding that these processes could improve modelling glacier evolution compared to observations (Ehrenfeucht et al., 2024). During this ungrounding process we find a change in the ocean meltwater currents as the ocean passageway opens, with the current switching direction and driving high melt rates upstream from the western pinning point. This process highlights the need to use coupled ice/ocean models to correctly model these feedbacks and interactions.

https://doi.org/10.5194/egusphere-2026-669
Preprint. Discussion started: 2 March 2026

It is likely that the effect of the ungrounding of this pinning point has been enhanced by the increase in ice shelf damage in western Thwaites that has been observed over the satellite era (Lhermitte et al., 2020). However, in the ocean plus damage forced simulations performed here, damage is applied immediately to floating ice with present day intensities and spatial pattern, whereas in reality Thwaites Ice Shelf has been observed to progressively become more damaged (Lhermitte et al., 2020), which likely started or at least increased after the 1940s ungrounding of the western pinning point, as visible in the 1973 imagery (figure 1a). Therefore, further work is required to fully understand the role of damage on the evolution of Thwaites grounding line as it retreats, ideally using a fully interactive ice damage model (e.g. Sun et al., 2017; Clayton et al., 2022). The historical western pinning point ungrounding is similar to a recurring process that has been modelled for Thwaites Glacier during the evolution of its future retreat (Bett et al., 2024). That process was found to be the key mechanism by which ocean warming can affect the rate of future ice loss, but no form of damage evolution was included in those projections, implying that the ice loss could be even more dramatic.

5.2 Eastern Thwaites

In our simulations, the ungrounding of the western Thwaites pinning point and the subsequent western grounding line retreat, leads to ice piracy of eastern Thwaites Glacier and ice shelf. This ice piracy may have starved the eastern part of the ice shelf and the eastern pinning point, helping to explain the observed thinning and breaking up of eastern Thwaites Ice Shelf, despite low melt rates in that area (Wild et al., 2024; Davis et al., 2023):. We have shown that the present-day spatial distribution of ice shelf damage, with a damaged western ice shelf and present-day location of the shear margin, increases the redirection of ice away from the eastern pinning point. This also matches with radar observations that indicate that Thwaites eastern pinning point had a greater extent in 1978 (Schroeder et al., 2019) compared to the present day, with Thwaites at that time having a more intact western ice shelf (Figure 1a) and 1978 being closer in time to the ungrounding of the western pinning point and therefore having less time for any ice piracy or redirection to have an effect.

Similarly, we have shown that ice piracy diverts ice away from the eastern grounding line, which may help to explain observed eastern Thwaites grounding line retreat (Rignot et al., 2014; Milillo et al., 2019), despite suppressed observed eastern melt rates (Davis et al., 2023). This historical reduced flow into the eastern Thwaites Ice Shelf, from flow diversion and deceleration, could be the primary driver of the observed retreat, as eastern Thwaites modelling finds it provides minimal buttressing in the present day (Gudmundsson et al., 2023). While piracy may have been the initial trigger of ice loss from eastern Thwaites, its future evolution will be influenced by melt rates (Davis et al., 2023), changes in damage (Wild et al., 2024) and perhaps by the predicted ungrounding of eastern Thwaites pinning point if it does provide any buttressing (Wild et al., 2022). Notably an example of ice piracy being an important process has recently been observed over similarly short timescales in the nearby Kohler Glacier (Selley et al., 2025). It appears that the retreat of Eastern Thwaites is separate to the retreat in the western trunk but is influenced by it, so that timings of the events for the western and eastern Thwaites likely need to be correct to recreate the observed shape of west/east retreat.

https://doi.org/10.5194/egusphere-2026-669
Preprint. Discussion started: 2 March 2026

5.3 Quasi-steady states and most plausible pre-1940s state:

We found three different quasi-steady grounding line positions for Thwaites Glacier, when a healed ice shelf is applied (Figure 8b). The sensitivity to two distinct model parameters (thermocline height and ice shelf damage) and the presence of three quasi-steady grounded areas hints at a complex underlying stability landscape that the Thwaites Glacier system occupied in the late twentieth century. Rather than a single tipping point at some definite thermocline height, Thwaites Glacier may have had multiple loci of tipping in the space defined by thermocline height and damage. It (Thom, 1975)seems clear that the simplest conceptual models of tipping such as cusp catastrophes, and even butterfly catastrophes ((Thom, 1975) may struggle to represent the complex behaviour revealed by our numerical simulations. Indeed, the search for quasi-steady states was not exhaustive, so it is possible there could be more. This demonstrates that the underlying stability landscape for Thwaites Glacier is not simple, and this glacier may exhibit a complex, non-linear response to climatic forcing.

In particular our results suggest that non-reversible transitions between quasi-steady states may play an important role in the historical retreat of Thwaites Glacier. For an ocean thermocline height corresponding to the present day mean (700 m depth), but with undamaged ice, the choice of which quasi-steady state the ice approaches depends upon the history of the glacier evolution. It is also notable that once the ice is damaged, all quasi-steady states disappear (Figure 8c). This implies that with its current damaged state, Thwaites Glacier has passed a qualitative threshold.

Having found these multiple quasi-steady states within our ice retreat simulations, we can now re-examine which of these three states is the most plausible pre-1940s state. Using the available evidence of sediment cores from Thwaites Glacier (Clark et al., 2024) and the 1947 aerial imagery (USGS, 2018) - we find that state 2 is potentially the best candidate for a pre-1940s Thwaites Glacier. The sediment core analysis suggests that there was an ocean passage upstream of the western pinning point prior to the 1940s (unlike in state 1, which was our original reference pre-1940s state) and that western grounding line retreat may have occurred in the 1950s (Clark et al., 2024) so suggesting an advanced grounding line position compared to the 1990s satellite observed grounding line position (unlike in state 3). This leaves state 2 as the most plausible pre-1940s Thwaites Glacier state that we have found.

We can now compare this best estimate of a quasi-steady pre-1940s modelled Thwaites state against the 1947 aerial imagery. Firstly, one of the key features of the aerial imagery is that the western ice shelf outflow does not match the location of the main western outflow shown in the 1973 satellite image. Now, examining the modelling results we find that state 2 (and indeed all three quasi-steady states) suggests that the main western outflow was shifted westward compared to the present-day configuration, due to the presence of the grounded western pinning point, in agreement with the 1947 photography (Figure 10a,b,c). However, the eastern edge of the western outflow is even more westward shifted in the observations than in the model. This may be due to the lack of a dynamical damage model in the simulation, as the aerial imagery shows large

https://doi.org/10.5194/egusphere-2026-669
Preprint. Discussion started: 2 March 2026

numbers of icebergs on the eastern edge (Figure 10 b,c) suggesting damage and calving on this edge, presumably due to the interaction with the historic western pinning point, where the damage/calving begins (Figure 11a). In contrast, the model state has healed ice. Despite this missing process the images show both edges of the modelled western outflow lining up with the 1947 photographs, much better than that of the outflow in the 1973 image. It should be noted that while this is a useful comparison to make, this imagery is taken close to the proposed time that the western pinning point ungrounded (Clark et al., 2024) and therefore Thwaites may already be in transition in this imagery and so not represent the true pre-1940s quasi-steady state.

https://doi.org/10.5194/egusphere-2026-669
Preprint. Discussion started: 2 March 2026

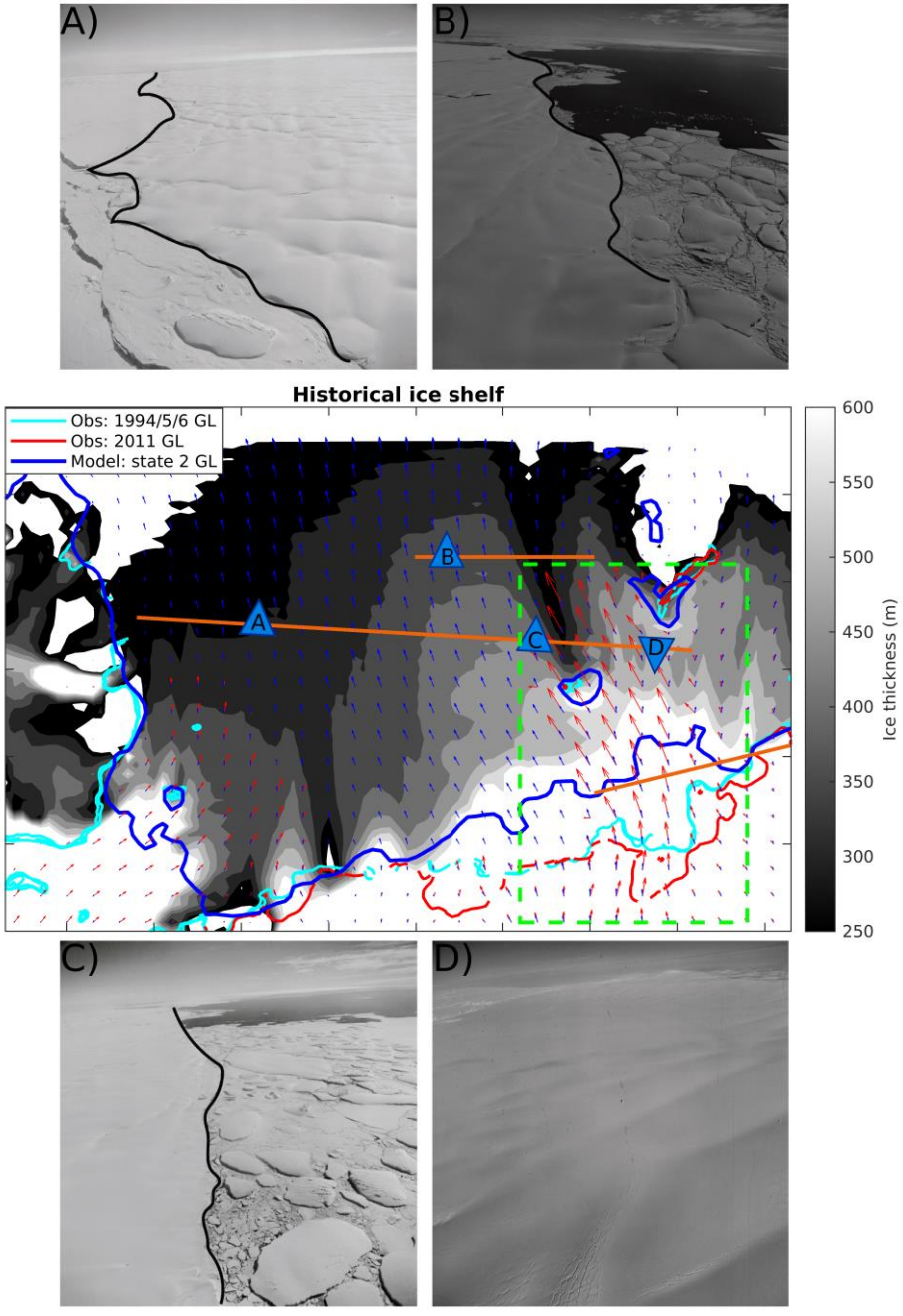

650 **Figure 10:** Ice velocities for quasi-steady state 2 (blue arrows) and for present day model (red arrows) over ice thickness of state 2 saturated between 250m and 600m. Plotted over approximate area shown in Figure 3a by red dashed box. Observed grounding lines for 1994/5/6 (cyan) and 2011 (red) are shown (Rignot et al., 2016). Orange lines show the three different flight lines from the U.S. Navy operation Highjump in 1947 (USGS, 2018). Snapshots taken along the flight paths at the indicated location and direction shown by orientation of the triangle. Aerial photograph in panel d, which were originally

https://doi.org/10.5194/egusphere-2026-669
Preprint. Discussion started: 2 March 2026

taken with a south-looking orientation from the place, have been horizontally mirrored to maintain a consistent orientation and facilitate direct visual alignment with panel (a, b, c) that were taken north-looking.

Secondly, the 1947 images also suggest that the shear margin was aligned with the historical western pinning point and then extended approximately south/south-eastward, rather than the present-day location which is aligned with the eastern pinning point (Figure 3d, Figure 10). While there is no dynamical damage model in these simulations, we can examine the maximum shear fields, derived from principal strain rates, for the different quasi-steady states, all with healed ice shelves (Figure 11), to estimate locations of potential shear margin formation. The maximum shear is calculated as half the difference between principal strain rates from the model.

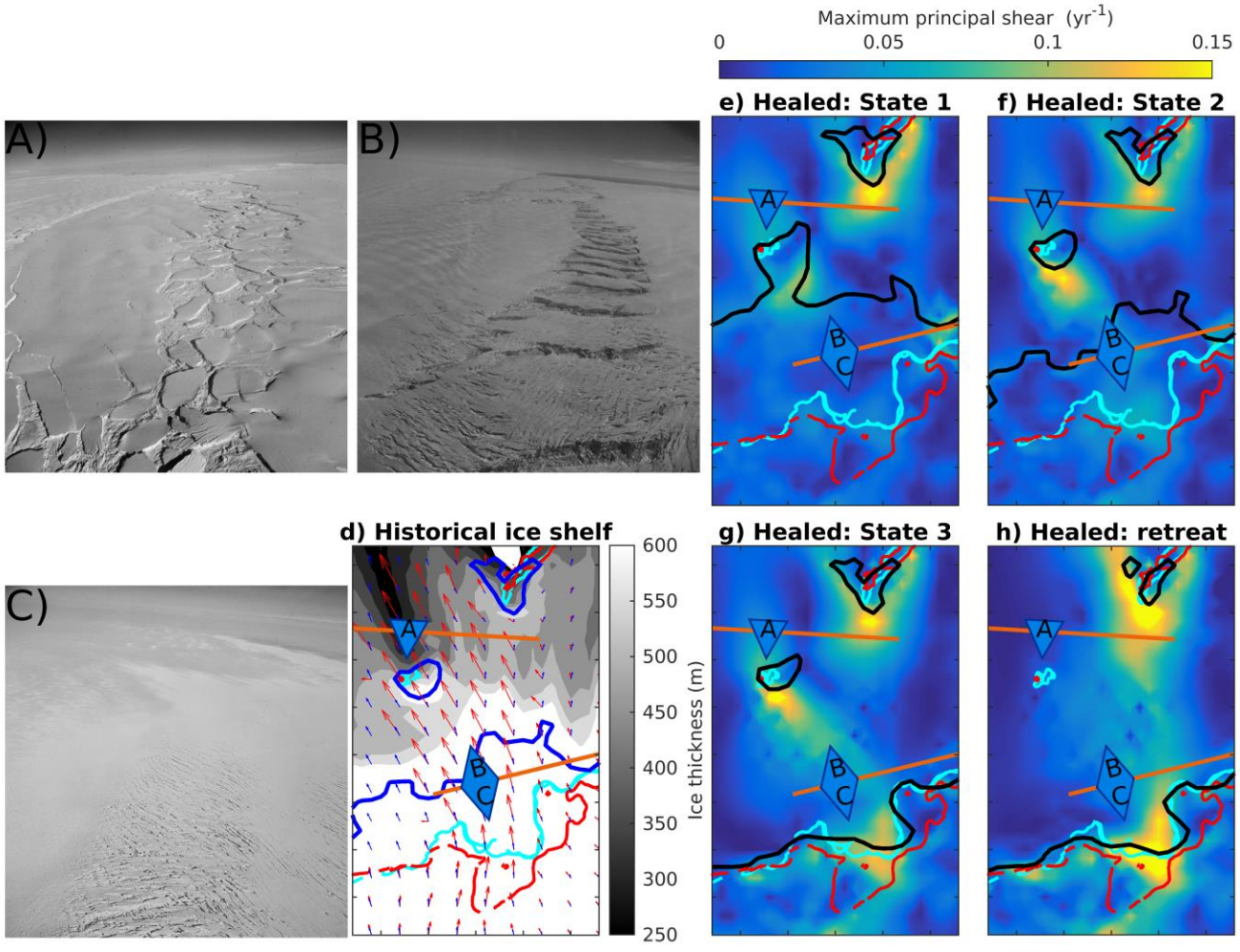

Figure 11: a,b,c) 1947 aerial images taken at indicted locations and direction shown by orientation of triangles in other panels. Aerial photograph in panel (a,c), which were originally taken with a south-looking orientation from the place, have

https://doi.org/10.5194/egusphere-2026-669
Preprint. Discussion started: 2 March 2026

been horizontally mirrored to maintain a consistent orientation and facilitate direct visual alignment with panel b that was taken north-looking. d) Zoom of green dashed box from Figure 10. e,f,g,h) Maximum shear for quasi-steady states 1-3 (e, f, g) and for snapshot of the retreating ocean forced only simulation with warm (600 m thermocline depth) forcing after the western pinning point ungrounding and retreat to near 1990s grounding position (~455 years, as examined in Figure 6) (h). Model grounding line (blue in (d), otherwise black), and observed grounding lines for 1994/5/6 (cyan) and 2011 (red) are shown (Rignot et al., 2016). Orange lines show two flight lines from the U.S. Navy operation Highjump in 1947 (USGS, 2018).

All three quasi-steady states have maximum shear on the ice shelf around both pinning points (Figure 11 e,f,g). South of the western pinning point there is a potential shear margin, which extends further southwards the further the grounding line retreats (Figure 11 c,d,g), which appears to match the location of a shear margin shown in the 1947 imagery (Figure 11). Crucially, when these fields are compared to the present-day configuration with the ungrounded western pinning point, shown here for a snapshot of the retreating ocean only forced case, we see a westward movement of the northern end of this shear margin to the familiar present-day shear margin position linked to the eastern pinning point (Figure 11h). These results explain the westward-shifted pre-1940s shear margin that existed until the ungrounding of the western pinning point. Additionally, the shear margin with a distinctive rifting pattern shown in the 1947 imagery appears to start at its intersection with the flight line (Figures 11b and 11c), which could suggest that the grounding line is located here at the time of the imagery, as other such recurring rifting features, for example in PIG, start near the grounding line (e.g. Lhermitte et al. (2020)). This would further support our inference that Thwaites is in a state 2 configuration in these images.

This shift in the outflow location and shear margin to the present-day configuration likely happens after the ungrounding of the western pinning point, as both the shear margin and main western outflow are near the present-day configuration in the earliest satellite image in 1973. This all suggests a fundamental change in the configuration of Thwaites Ice Shelf has occurred from the 1940s to the present day and even before the 1973 satellite image.

In this study, most simulations were run forward from state 1, since that is the most advanced state we could achieve (with healed ice damage and cold ocean conditions). However, we subsequently found that multiple quasi-steady states exist and that state 2 is a more plausible candidate for a pre-1940s state of Thwaites Glacier. This may help to explain differences in timings between our simulations and the observed retreat. However, this study is not intended as a full hindcast of Thwaites Glacier, due additionally to our simplified treatment of damage and ocean thermocline forcings. Instead, this study focuses on understanding the key processes and stability landscape of Thwaites Glacier. Future work is required to incorporate these insights and assess how well new simulations match observed Thwaites retreat in a hindcast-focused study.

https://doi.org/10.5194/egusphere-2026-669
Preprint. Discussion started: 2 March 2026

The three different quasi-steady states we found are expected to have different vulnerabilities of western pinning point ungrounding to ocean forcing, depending on whether the ocean passageway is open upstream of the pinning point or not. This could affect the resilience of the system to climatic events like the 1940s event that may have triggered the current retreat. Such events are estimated to have occurred several times in the last 10,000 years (O'connor et al., 2023), while Thwaites Glacier is estimated to have been within 45 km of its present-day grounding line and having had only minor oscillations in grounding line position during this time (Clark et al., 2024). It is possible that Thwaites Glacier happened to be in a position where the pinning point was not exposed to high melt rates upstream of it, reducing the impact of some previous 1940s-like climatic events, or Thwaites Glacier could have ungrounded from the western pinning point during warm anomalies and subsequently recovered during cooler climatic periods. This suggests several possibilities, including i) after the ungrounding in the 1940s, anthropogenic trends in oceanic forcings later in the 20th century could have played a role in contributing to the lack of recovery of the western pinning point; ii) there are further unknown features to the 1940s event which make it a more extreme and rare event, such as longer-period warm anomalies underlying the 1940s warm years or iii) the 1940s event may have combined with longer time-scale natural processes like gradual snowfall starvation or ocean forcing trends, which could have widened the channel upstream of the pinning point over previous centuries or millennia and pre-conditioned the system for the post-1940s retreat. These considerations have been proposed previously (Holland et al., 2022; O'connor et al., 2023), but our new insight into the sensitivities of the different steady states reveals how subtle changes in the ice state can have large impacts on their response to climatic forcing, such as anthropogenic trends in warming (Holland et al., 2019).

5.4 Damage and stability

The warmest modelled ocean forcing causes Thwaites Glacier to pass through the three quasi-steady states and retreat past the present-day grounding line, even with a healed ice shelf. In addition, applying the present-day spatial distribution of damage to the evolving floating ice causes the ice to retreat for all modelled ocean forcings, and removes the existence of the healed-ice quasi-steady states. These results suggest that the present-day ice shelf damage reflects a fundamental change in the system that has removed any possibility of the ice stream stabilising or regrowing. This cautions against assuming that Thwaites Glacier, with its current damaged configuration, was close to equilibrium for cooler ocean forcings (e.g. Reese et al. (2023) and Hill et al. (2023)). However, in this study we only consider one initialisation for the present-day ice damage field from one model, and further work is required to test the robustness of these results over multiple possible initialisations and models, ideally using a fully evolving physics-based damage model.

This suggestion of the importance of damage links with a previous study where Thwaites Glacier retreats for the extreme case of no ice shelf melting, using this model with its present-day geometrical configuration and highly damaged western ice shelf (Williams et al., 2026; Bett et al., 2024). This work also explains the result that the present-day Thwaites Ice Shelf provides minimal buttressing, such that its removal has limited impact on the future trajectory of Thwaites (Gudmundsson et

https://doi.org/10.5194/egusphere-2026-669
Preprint. Discussion started: 2 March 2026

al., 2023). Both studies are explained by our finding that Thwaites is experiencing ongoing adjustment due to the historic changes in buttressing that occurred during the 20th century. The ungrounding of the western pinning point and damage feedbacks have already moved Thwaites away from the quasi-steady states that it might otherwise have achieved. Therefore, our results suggest that the present-day retreat is being driven at least partially by a historical change, which other studies have noted as an option (Gudmundsson et al., 2023; Joughin et al., 2014). However, the rate of ice loss from Thwaites Glacier remains sensitive to ocean forcing over the longer term, as demonstrated by the more rapid ice loss in the higher-thermocline cases. As a result, Thwaites Glacier is likely also being impacted to some extent by anthropogenic trends in forcings in the present day, which will increasingly become a stronger influence into the future with modelled oceanic warming trends (Naughten et al., 2023).

Crucially, our results suggest that any stabilisation of Thwaites Glacier near its current grounding line would require intact, undamaged ice to reground on the western pinning point, rather than just the simple direct thickening of existing damaged ice by reduced melt rates due to a cooling of the ocean. This process could have potentially occurred before, where Thwaites Glacier, as inferred through observations near Crosson Ice shelf, has been suggested to have thinned to a below present-day thickness in the mid Holocene before recovering in the Late Holocene (Nichols et al., 2024). During this process the ice shelf could have become damaged like in the present day and then reformed, or a slower retreat could have occurred, maintaining a sufficiently intact ice shelf and pinning point throughout any retreat and re-advance. It is possible that the extent of Thwaites Ice Shelf directly impacts the buttressing provided by Crosson Ice shelf and vice versa. These ice shelves don't interact in the present-day configuration but appear to be connected in the 1946-47s imagery and could have had a greater connection before that if this imagery indeed shows Thwaites Ice Shelf already in transition. However, any processes leading to the potential recovery of a damaged ice shelf are currently very poorly understood, with future work required to understand the dynamical interactions between melt rates, ice damage and ice dynamics. In this study we find that simply prescribing the healing of the floating ice shelf in the present-day state allows for a regrounding of the western pinning point in an extreme no-melt case to provide sufficient buttressing for the main grounding line to re-advance onto the bathymetric high. Indeed, we have shown that this advance can occur from grounding line positions that are similar to the present day (i.e. state 3) for the cold ocean forcings of 900m and 800m thermocline depths and can be quasi-steady in this position with a 700m thermocline depth, if the ice shelf damage is instantly healed.

These results all highlight a key limitation of this study, which is that damage evolution is not represented by a dynamical physical model. Here, instead we apply damage as a forcing alongside ocean forcing, which has the disadvantage of disabling interactions between ice shelf melting, damage and ice dynamics. This requires us to make several assumptions, such as selecting damage values for the ice shelf outside the current floating area, suddenly enabling and disabling damage in our simulations, enabling damage on floating ice as the grounding line retreats, and not changing damage upstream of the modern grounding line. Our results highlight the importance of ice damage and so these choices are likely to be influential.

https://doi.org/10.5194/egusphere-2026-669
Preprint. Discussion started: 2 March 2026

Therefore, future work is needed to model the dynamical interactions and feedbacks between ice shelf melting, ice damage, ice dynamics and pinning point ungrounding.

6. Conclusions

In this study we present 20th century historical ice/ocean coupled simulations of Thwaites Glacier, exploring its stability, retreat, and processes related to ocean melting and ice damage. The findings are validated against a 1973 satellite image and a new analysis of aerial photographs of Thwaites Ice Shelf from 1946-47. These observations show that prior to the 1940s Thwaites Glacier had a large western intact ice tongue which is shifted westward compared to the present-day western ice shelf.

The first step in the modelling is to create an initial quasi-steady reference pre-1940s Thwaites Glacier configuration, which is challenging because we start from a present-day model initialisation which retreats even in an extreme case of zero ocean melting. We find that healing the ice damage on western Thwaites Ice Shelf and extending the static ice front are needed, both supported by observations, so that the buttressing provided by a regrounded western pinning point is sufficient to create an initial advanced quasi-steady state.

The next step is to run simulations of Thwaites Glacier retreat from this reference pre-1940s state, under different ocean forcings and ice damage conditions. These simulations highlight several key processes and events in the retreat of Thwaites Glacier. The initial trigger is the opening of an ocean channel on the upstream side of the western pinning point, which allows warm ocean waters to melt and thin the ice supplied to the pinning point. The ensuing ungrounding and loss of buttressing leads to rapid acceleration and retreat. This rapid acceleration led to increasing damage, thinning and weakening the ice shelf and so preventing any regrounding of the western pinning point. After this, the transient effect of ice piracy leads to ice starvation in both the eastern Thwaites Ice Shelf, including the eastern pinning point, and the eastern Thwaites Glacier. This may help explain the observed present-day eastern Thwaites grounding line retreat, despite being located on a bathymetric high, with only low melt rates present.

Finally, by conducting a set of simulations with different ocean forcings and damage states, we show that multiple quasi-steady grounding line positions can exist for Thwaites Glacier. When considering fully healed damage, we find 3 separate quasi-steady states for the same ocean forcing, which approximates average present-day conditions. However, sufficient damage and/or ocean forcing prevents the glacier from remaining in these states. With healed damage, colder conditions lead to advance to the most advanced state and the warmest conditions retreat Thwaites Glacier outside of the considered area. Crucially, when forced with the present-day ice shelf damage to the evolving floating ice, Thwaites retreats through all of

https://doi.org/10.5194/egusphere-2026-669
Preprint. Discussion started: 2 March 2026

these potential steady states and past the present grounding line, for all simulated ocean conditions. This implies that the damage now inherent in Thwaites Glacier has qualitatively decreased its ability to recover from the ongoing retreat.

Out of these quasi-steady states, the state we name "state 2" is a good candidate for a pre-1940s state that matches the available observations for Thwaites Glacier, with an advanced grounding line compared to the present day, but with an ocean passage-way already open upstream of the western pinning point. The main ice outflow in all these historical states is shifted to the west of the present-day outflow, due to ice flow blocking by the western pinning point, which matches observations from 1947 aerial images of Thwaites Ice Shelf.

Now that we have a better idea of the processes controlling the historical evolution of Thwaites Glacier, we may start to isolate the climatic forcings that drove the ongoing retreat and consider how they may evolve in future.

Code and data availability

The version of MITgcm used in this study is available at https://github.com/David-Bett4/MITgcm/tree/Coupling_wHoriz_lat_Pchild_new_divout (commit 26ffb9f, last access: 30 May 2024) and https://doi.org/10.5281/zenodo.11394744 (Campin et al., 2024). The version of WAVI used in this study is available at https://github.com/David-Bett4/WAVI.jl/tree/MITgcm_coupling (commit 7c292f1, last access: 30 May 2024) and https://doi.org/10.5281/zenodo.11389948 (Bradley et al., 2024). Coupling scripts and model input text files are available at https://github.com/David-Bett4/20th_Cent_THW_MITgcm_WAVI_coupling and will be available on Zenodo upon publication of the paper. The model output underlying the figures and calculations in this paper will be available through the UK Polar Data Centre upon publication of the paper.

Author contributions

DTB set up ocean initial state, implemented idealised damage system, ran coupled simulations, performed analysis and led the manuscript writing. CRW set up initial WAVI present day ice model states and performed WAVI ice model relaxation simulations. RJA, PRH, CRW designed and supervised the project. BWM prepared, plotted and helped analyse aerial and satellite imagery. All of the co-authors contributed to experiment design and editing the manuscript.

Competing interests

The contact author has declared that none of the authors has any competing interests.

https://doi.org/10.5194/egusphere-2026-669
Preprint. Discussion started: 2 March 2026

Acknowledgements

This work used the ARCHER2 UK National Supercomputing Service (https://www.archer2.ac.uk, last access: 22/09/25).

Financial support

This publication was supported by PROTECT. This project has received funding from the European Union's Horizon 2020 research and innovation programme (grant no. 869304), PROTECT contribution number XX. This research was supported by Ocean Cryosphere Exchanges in ANtarctica: Impacts on Climate and the Earth system, OCEAN ICE, which is funded by the European Union, Horizon Europe Funding Programme for research and innovation under grant agreement Nr. 101060452, 10.3030/101060452. OCEAN ICE contribution number XX. This work was funded by UK Research and Innovation (UKRI) under the UK government's Horizon Europe funding Guarantee [grant number 10048443].

References

Arthern, R. J. and Williams, C. R.: The sensitivity of West Antarctica to the submarine melting feedback, Geophysical Research Letters, 44, 2352-2359, https://doi.org/10.1002/2017GL072514, 2017.

Arthern, R. J., Hindmarsh, R. C. A., and Williams, C. R.: Flow speed within the Antarctic ice sheet and its controls inferred from satellite observations, Journal of Geophysical Research: Earth Surface, 120, 1171-1188, https://doi.org/10.1002/2014JF003239, 2015.

Bett, D. T., Bradley, A. T., Williams, C. R., Holland, P. R., Arthern, R. J., and Goldberg, D. N.: Coupled ice–ocean interactions during future retreat of West Antarctic ice streams in the Amundsen Sea sector, The Cryosphere, 18, 2653-2675, 10.5194/tc-18-2653-2024, 2024.

Bradley, A. T. and Hewitt, I. J.: Tipping point in ice-sheet grounding-zone melting due to ocean water intrusion, Nature Geoscience, 17, 631-637, 10.1038/s41561-024-01465-7, 2024.

Bradley, A. T., Bett, D. T., Williams, C. R., Arthern, R. J., Holland, P. R., Bryne, J., and Edwards, T. L.: Quantifying and attributing the role of anthropogenic climate change in industrial-era retreat of Pine Island Glacier, EGUsphere, 2025, 1-31, 10.5194/egusphere-2025-2315, 2025.

Bryan, K., Manabe, S., and Pacanowski, R. C.: A global ocean-atmosphere climate model. Part II. The oceanic circulation, Journal of Physical Oceanography, 5, 30-46, 1975.

Cazenave, A., Palanisamy, H., and Ablain, M.: Contemporary sea level changes from satellite altimetry: What have we learned? What are the new challenges?, Advances in Space Research, 62, 1639-1653, https://doi.org/10.1016/j.asr.2018.07.017, 2018.

Clark, R. W., Wellner, J. S., Hillenbrand, C.-D., Totten, R. L., Smith, J. A., Miller, L. E., Larter, R. D., Hogan, K. A., Graham, A. G. C., Nitsche, F. O., Lehrmann, A. A., Lepp, A. P., Kirkham, J. D., Fitzgerald, V. T., Garcia-Barrera, G., Ehrmann, W., and Wacker, L.: Synchronous retreat of Thwaites and Pine Island glaciers in response to external forcings in the presatellite era, Proceedings of the National Academy of Sciences, 121, e2211711120, doi:10.1073/pnas.2211711120, 2024.

Clayton, T., Duddu, R., Siegert, M., and Martínez-Pañeda, E.: A stress-based poro-damage phase field model for hydrofracturing of creeping glaciers and ice shelves, Engineering Fracture Mechanics, 272, 108693, https://doi.org/10.1016/j.engfracmech.2022.108693, 2022.

Conway, H., Catania, G., Raymond, C. F., Gades, A. M., Scambos, T. A., and Engelhardt, H.: Switch of flow direction in an Antarctic ice stream, Nature, 419, 465-467, 10.1038/nature01081, 2002.

Davis, P. E. D., Nicholls, K. W., Holland, D. M., Schmidt, B. E., Washam, P., Riverman, K. L., Arthern, R. J., Vaňková, I., Eayrs, C., Smith, J. A., Anker, P. G. D., Mullen, A. D., Dichek, D., Lawrence, J. D., Meister, M. M., Clyne, E., Basinski-

https://doi.org/10.5194/egusphere-2026-669
Preprint. Discussion started: 2 March 2026

Ferris, A., Rignot, E., Queste, B. Y., Boehme, L., Heywood, K. J., Anandakrishnan, S., and Makinson, K.: Suppressed basal melting in the eastern Thwaites Glacier grounding zone, Nature, 614, 479-485, 10.1038/s41586-022-05586-0, 2023.
De Rydt, J. and Naughten, K.: Geometric amplification and suppression of ice-shelf basal melt in West Antarctica, The Cryosphere, 18, 1863-1888, 10.5194/tc-18-1863-2024, 2024.
De Rydt, J., Reese, R., Paolo, F. S., and Gudmundsson, G. H.: Drivers of Pine Island Glacier speed-up between 1996 and 2016, The Cryosphere, 15, 113-132, 10.5194/tc-15-113-2021, 2021.
Dutrieux, P., De Rydt, J., Jenkins, A., Holland, P. R., Ha, H. K., Lee, S. H., Steig, E. J., Ding, Q., Abrahamsen, E. P., and Schröder, M.: Strong Sensitivity of Pine Island Ice-Shelf Melting to Climatic Variability, Science, 343, 174-178, 10.1126/science.1244341, 2014.
Ehrenfeucht, S., Rignot, E., and Morlighem, M.: Seawater Intrusion in the Observed Grounding Zone of Petermann Glacier Causes Extensive Retreat, Geophysical Research Letters, 51, e2023GL107571, https://doi.org/10.1029/2023GL107571, 2024.
Ferrigno, J. G., Lucchitta, B. K., Mullins, K. F., Allison, A. L., Allen, R. J., and Gould, W. G.: Velocity measurements and changes in position of Thwaites Glacier/iceberg tongue from aerial photography, Landsat images and NOAA AVHRR data, Annals of Glaciology, 17, 239-244, 10.3189/S0260305500012908, 1993.
Gudmundsson, G. H., Barnes, J. M., Goldberg, D. N., and Morlighem, M.: Limited Impact of Thwaites Ice Shelf on Future Ice Loss From Antarctica, Geophysical Research Letters, 50, e2023GL102880, https://doi.org/10.1029/2023GL102880, 2023.
Hill, E. A., Urruty, B., Reese, R., Garbe, J., Gagliardini, O., Durand, G., Gillet-Chaulet, F., Gudmundsson, G. H., Winkelmann, R., Chekki, M., Chandler, D., and Langebroek, P. M.: The stability of present-day Antarctic grounding lines – Part 1: No indication of marine ice sheet instability in the current geometry, The Cryosphere, 17, 3739-3759, 10.5194/tc-17-3739-2023, 2023.
Holland, P. R., Bevan, S. L., and Luckman, A. J.: Strong Ocean Melting Feedback During the Recent Retreat of Thwaites Glacier, Geophysical Research Letters, 50, e2023GL103088, https://doi.org/10.1029/2023GL103088, 2023.
Holland, P. R., Bracegirdle, T. J., Dutrieux, P., Jenkins, A., and Steig, E. J.: West Antarctic ice loss influenced by internal climate variability and anthropogenic forcing, Nature Geoscience, 12, 718-724, 10.1038/s41561-019-0420-9, 2019.
Holland, P. R., O'Connor, G. K., Bracegirdle, T. J., Dutrieux, P., Naughten, K. A., Steig, E. J., Schneider, D. P., Jenkins, A., and Smith, J. A.: Anthropogenic and internal drivers of wind changes over the Amundsen Sea, West Antarctica, during the 20th and 21st centuries, The Cryosphere, 16, 5085-5105, 10.5194/tc-16-5085-2022, 2022.
Joughin, I., Smith, B. E., and Medley, B.: Marine Ice Sheet Collapse Potentially Under Way for the Thwaites Glacier Basin, West Antarctica, Science, 344, 735-738, 10.1126/science.1249055, 2014.
Larter, R. D., Anderson, J. B., Graham, A. G. C., Gohl, K., Hillenbrand, C.-D., Jakobsson, M., Johnson, J. S., Kuhn, G., Nitsche, F. O., Smith, J. A., Witus, A. E., Bentley, M. J., Dowdeswell, J. A., Ehrmann, W., Klages, J. P., Lindow, J., Cofaigh, C. Ó., and Spiegel, C.: Reconstruction of changes in the Amundsen Sea and Bellingshausen Sea sector of the West Antarctic Ice Sheet since the Last Glacial Maximum, Quaternary Science Reviews, 100, 55-86, https://doi.org/10.1016/j.quascirev.2013.10.016, 2014.
Lhermitte, S., Sun, S., Shuman, C., Wouters, B., Pattyn, F., Wuite, J., Berthier, E., and Nagler, T.: Damage accelerates ice shelf instability and mass loss in Amundsen Sea Embayment, Proceedings of the National Academy of Sciences, 117, 24735-24741, doi:10.1073/pnas.1912890117, 2020.
McCormack, F. S., Roberts, J. L., Kulessa, B., Aitken, A., Dow, C. F., Bird, L., Galton-Fenzi, B. K., Hochmuth, K., Jones, R. S., Mackintosh, A. N., and McArthur, K.: Assessing the potential for ice flow piracy between the Totten and Vanderford glaciers, East Antarctica, The Cryosphere, 17, 4549-4569, 10.5194/tc-17-4549-2023, 2023.
Miles, B. W. J. and Bingham, R. G.: Progressive unanchoring of Antarctic ice shelves since 1973, Nature, 626, 785-791, 10.1038/s41586-024-07049-0, 2024.
Miles, B. W. J., Stokes, C. R., Jenkins, A., Jordan, J. R., Jamieson, S. S. R., and Gudmundsson, G. H.: Intermittent structural weakening and acceleration of the Thwaites Glacier Tongue between 2000 and 2018, Journal of Glaciology, 66, 485-495, 10.1017/jog.2020.20, 2020.
Milillo, P., Rignot, E., Rizzoli, P., Scheuchl, B., Mouginot, J., Bueso-Bello, J., and Prats-Iraola, P.: Heterogeneous retreat and ice melt of Thwaites Glacier, West Antarctica, Science Advances, 5, eaau3433, 10.1126/sciadv.aau3433, 2019.
Morlighem, M.: MEaSUREs BedMachine Antarctica, Version 3 [dataset], https://doi.org/10.5067/FPSU0V1MWUB6, 2022.

https://doi.org/10.5194/egusphere-2026-669
Preprint. Discussion started: 2 March 2026

Morlighem, M., Rignot, E., Binder, T., Blankenship, D., Drews, R., Eagles, G., Eisen, O., Ferraccioli, F., Forsberg, R., Fretwell, P., Goel, V., Greenbaum, J. S., Gudmundsson, H., Guo, J., Helm, V., Hofstede, C., Howat, I., Humbert, A., Jokat, W., Karlsson, N. B., Lee, W. S., Matsuoka, K., Millan, R., Mouginot, J., Paden, J., Pattyn, F., Roberts, J., Rosier, S., Ruppel, A., Seroussi, H., Smith, E. C., Steinhage, D., Sun, B., Broeke, M. R. v. d., Ommen, T. D. v., Wessem, M. v., and Young, D. A.: Deep glacial troughs and stabilizing ridges unveiled beneath the margins of the Antarctic ice sheet, Nature Geoscience, 13, 132-137, 10.1038/s41561-019-0510-8, 2020.

Mouginot, J., Rignot, E., and Scheuchl, B.: Sustained increase in ice discharge from the Amundsen Sea Embayment, West Antarctica, from 1973 to 2013, Geophysical Research Letters, 41, 1576-1584, https://doi.org/10.1002/2013GL059069, 2014.

Mouginot, J., Scheuchl, B., and Rignot, E.: MEaSUREs Annual Antarctic Ice Velocity Maps, Version 1 [dataset], https://doi.org/10.5067/9T4EPQXTJYW9, 2017a.

Mouginot, J., Rignot, E., Scheuchl, B., and Millan, R.: Comprehensive Annual Ice Sheet Velocity Mapping Using Landsat-8, Sentinel-1, and RADARSAT-2 Data, 10.3390/rs9040364, 2017b.

Nakayama, Y., Manucharyan, G., Zhang, H., Dutrieux, P., Torres, H. S., Klein, P., Seroussi, H., Schodlok, M., Rignot, E., and Menemenlis, D.: Pathways of ocean heat towards Pine Island and Thwaites grounding lines, Scientific Reports, 9, 16649, 10.1038/s41598-019-53190-6, 2019.

Naughten, K. A., Holland, P. R., and De Rydt, J.: Unavoidable future increase in West Antarctic ice-shelf melting over the twenty-first century, Nature Climate Change, 13, 1222-1228, 10.1038/s41558-023-01818-x, 2023.

Naughten, K. A., Holland, P. R., Dutrieux, P., Kimura, S., Bett, D. T., and Jenkins, A.: Simulated Twentieth-Century Ocean Warming in the Amundsen Sea, West Antarctica, Geophysical Research Letters, 49, e2021GL094566, https://doi.org/10.1029/2021GL094566, 2022.

Nias, I. J., Cornford, S. L., Edwards, T. L., Gourmelen, N., and Payne, A. J.: Assessing Uncertainty in the Dynamical Ice Response to Ocean Warming in the Amundsen Sea Embayment, West Antarctica, Geophysical Research Letters, 46, 11253-11260, https://doi.org/10.1029/2019GL084941, 2019.

Nichols, K. A., Adams, J. R., Brown, K., Creel, R. C., McKenzie, M. A., Venturelli, R. A., Johnson, J. S., Rood, D. H., Wilcken, K., Woodward, J., and Roberts, S. J.: Direct Geologic Constraints on the Timing of Late Holocene Ice Thickening in the Amundsen Sea Embayment, Antarctica, Geophysical Research Letters, 51, e2024GL110350, https://doi.org/10.1029/2024GL110350, 2024.

O'Connor, G. K., Holland, P. R., Steig, E. J., Dutrieux, P., and Hakim, G. J.: Characteristics and rarity of the strong 1940s westerly wind event over the Amundsen Sea, West Antarctica, The Cryosphere, 17, 4399-4420, 10.5194/tc-17-4399-2023, 2023.

Reed, B., Green, J. A. M., Jenkins, A., and Gudmundsson, G. H.: Recent irreversible retreat phase of Pine Island Glacier, Nature Climate Change, 14, 75-81, 10.1038/s41558-023-01887-y, 2024.

Reese, R., Garbe, J., Hill, E. A., Urruty, B., Naughten, K. A., Gagliardini, O., Durand, G., Gillet-Chaulet, F., Gudmundsson, G. H., Chandler, D., Langebroek, P. M., and Winkelmann, R.: The stability of present-day Antarctic grounding lines – Part 2: Onset of irreversible retreat of Amundsen Sea glaciers under current climate on centennial timescales cannot be excluded, The Cryosphere, 17, 3761-3783, 10.5194/tc-17-3761-2023, 2023.

Rignot, E., Mouginot, J., and Scheuchl, B.: MEaSUREs Antarctic Grounding Line from Differential Satellite Radar Interferometry, Version 2, NASA National Snow and Ice Data Center Distributed Active Archive Center [dataset], 10.5067/IKBWW4RYHF1Q, 2016.

Rignot, E., Mouginot, J., Morlighem, M., Seroussi, H., and Scheuchl, B.: Widespread, rapid grounding line retreat of Pine Island, Thwaites, Smith, and Kohler glaciers, West Antarctica, from 1992 to 2011, Geophysical Research Letters, 41, 3502-3509, https://doi.org/10.1002/2014GL060140, 2014.

Rignot, E., Ciracì, E., Scheuchl, B., Tolpekin, V., Wollersheim, M., and Dow, C.: Widespread seawater intrusions beneath the grounded ice of Thwaites Glacier, West Antarctica, Proceedings of the National Academy of Sciences, 121, e2404766121, 10.1073/pnas.2404766121, 2024.

Rignot, E., Mouginot, J., Scheuchl, B., van den Broeke, M., van Wessem, M. J., and Morlighem, M.: Four decades of Antarctic Ice Sheet mass balance from 1979–2017, Proceedings of the National Academy of Sciences, 116, 1095-1103, doi:10.1073/pnas.1812883116, 2019.

https://doi.org/10.5194/egusphere-2026-669
Preprint. Discussion started: 2 March 2026

Schroeder, D. M., Dowdeswell, J. A., Siegert, M. J., Bingham, R. G., Chu, W., MacKie, E. J., Siegfried, M. R., Vega, K. I., Emmons, J. R., and Winstein, K.: Multidecadal observations of the Antarctic ice sheet from restored analog radar records, Proceedings of the National Academy of Sciences, 116, 18867-18873, 10.1073/pnas.1821646116, 2019.

Selley, H. L., Hogg, A. E., Davison, B. J., Dutrieux, P., and Slater, T.: Speed-up, slowdown, and redirection of ice flow on neighbouring ice streams in the Pope, Smith, and Kohler region of West Antarctica, The Cryosphere, 19, 1725-1738, 10.5194/tc-19-1725-2025, 2025.

Seroussi, H. and Morlighem, M.: Representation of basal melting at the grounding line in ice flow models, The Cryosphere, 12, 3085-3096, 10.5194/tc-12-3085-2018, 2018.

Seroussi, H., Nowicki, S., Payne, A. J., Goelzer, H., Lipscomb, W. H., Abe-Ouchi, A., Agosta, C., Albrecht, T., Asay-Davis, X., Barthel, A., Calov, R., Cullather, R., Dumas, C., Galton-Fenzi, B. K., Gladstone, R., Golledge, N. R., Gregory, J. M., Greve, R., Hattermann, T., Hoffman, M. J., Humbert, A., Huybrechts, P., Jourdain, N. C., Kleiner, T., Larour, E., Leguy, G. R., Lowry, D. P., Little, C. M., Morlighem, M., Pattyn, F., Pelle, T., Price, S. F., Quiquet, A., Reese, R., Schlegel, N. J., Shepherd, A., Simon, E., Smith, R. S., Straneo, F., Sun, S., Trusel, L. D., Van Breedam, J., van de Wal, R. S. W., Winkelmann, R., Zhao, C., Zhang, T., and Zwinger, T.: ISMIP6 Antarctica: a multi-model ensemble of the Antarctic ice sheet evolution over the 21st century, The Cryosphere, 14, 3033-3070, 10.5194/tc-14-3033-2020, 2020.

Shepherd, A., Wingham, D., and Rignot, E.: Warm ocean is eroding West Antarctic Ice Sheet, Geophysical Research Letters, 31, https://doi.org/10.1029/2004GL021106, 2004.

Shepherd, A., Gilbert, L., Muir, A. S., Konrad, H., McMillan, M., Slater, T., Briggs, K. H., Sundal, A. V., Hogg, A. E., and Engdahl, M. E.: Trends in Antarctic Ice Sheet Elevation and Mass, Geophysical Research Letters, 46, 8174-8183, https://doi.org/10.1029/2019GL082182, 2019.

Shepherd, A., Ivins, E., Rignot, E., Smith, B., van den Broeke, M., Velicogna, I., Whitehouse, P., Briggs, K., Joughin, I., Krinner, G., Nowicki, S., Payne, T., Scambos, T., Schlegel, N., A, G., Agosta, C., Ahlstrøm, A., Babonis, G., Barletta, V., Blazquez, A., Bonin, J., Csatho, B., Cullather, R., Felikson, D., Fettweis, X., Forsberg, R., Gallee, H., Gardner, A., Gilbert, L., Groh, A., Gunter, B., Hanna, E., Harig, C., Helm, V., Horvath, A., Horwath, M., Khan, S., Kjeldsen, K. K., Konrad, H., Langen, P., Lecavalier, B., Loomis, B., Luthcke, S., McMillan, M., Melini, D., Mernild, S., Mohajerani, Y., Moore, P., Mouginot, J., Moyano, G., Muir, A., Nagler, T., Nield, G., Nilsson, J., Noel, B., Otosaka, I., Pattle, M. E., Peltier, W. R., Pie, N., Rietbroek, R., Rott, H., Sandberg-Sørensen, L., Sasgen, I., Save, H., Scheuchl, B., Schrama, E., Schröder, L., Seo, K.-W., Simonsen, S., Slater, T., Spada, G., Sutterley, T., Talpe, M., Tarasov, L., van de Berg, W. J., van der Wal, W., van Wessem, M., Vishwakarma, B. D., Wiese, D., Wouters, B., and The, I. t.: Mass balance of the Antarctic Ice Sheet from 1992 to 2017, Nature, 558, 219-222, 10.1038/s41586-018-0179-y, 2018.

Smith, B., Fricker, H. A., Gardner, A. S., Medley, B., Nilsson, J., Paolo, F. S., Holschuh, N., Adusumilli, S., Brunt, K., Csatho, B., Harbeck, K., Markus, T., Neumann, T., Siegfried, M. R., and Zwally, H. J.: Pervasive ice sheet mass loss reflects competing ocean and atmosphere processes, Science, 368, 1239-1242, 10.1126/science.aaz5845, 2020.

Smith, J. A., Andersen, T. J., Shortt, M., Gaffney, A. M., Truffer, M., Stanton, T. P., Bindschadler, R., Dutrieux, P., Jenkins, A., Hillenbrand, C. D., Ehrmann, W., Corr, H. F. J., Farley, N., Crowhurst, S., and Vaughan, D. G.: Sub-ice-shelf sediments record history of twentieth-century retreat of Pine Island Glacier, Nature, 541, 77-80, 10.1038/nature20136, 2017.

Sun, S., Cornford, S. L., Moore, J. C., Gladstone, R., and Zhao, L.: Ice shelf fracture parameterization in an ice sheet model, The Cryosphere, 11, 2543-2554, 10.5194/tc-11-2543-2017, 2017.

Surawy-Stepney, T., Hogg, A. E., Cornford, S. L., and Davison, B. J.: Episodic dynamic change linked to damage on the Thwaites Glacier Ice Tongue, Nature Geoscience, 16, 37-43, 10.1038/s41561-022-01097-9, 2023.

Thom, R.: Structural stability and morphogenesis; an outline of a general theory of models, 1975.

Trevers, M., Cornford, S. L., Payne, A. J., Gasson, E., and Bevan, S. L.: Retreat of Thwaites Glacier Triggered by its Neighbours, 10.22541/essoar.170957499.97583808/v1, 2024.

Turner, K. A., Naughten, K. A., Holland, P. R., and Naveira Garabato, A. C.: Modeled Centennial Ocean Warming in the Amundsen Sea Driven by Thermodynamic Atmospheric Changes, Not Winds, Geophysical Research Letters, 52, e2024GL112287, https://doi.org/10.1029/2024GL112287, 2025.

USGS: USGS EROS Archive - Aerial Photography - Antarctic Single Frame Records [dataset], https://doi.org/10.5066/F7MW2FDP, 2018.

Wild, C. T., Alley, K. E., Muto, A., Truffer, M., Scambos, T. A., and Pettit, E. C.: Weakening of the pinning point buttressing Thwaites Glacier, West Antarctica, The Cryosphere, 16, 397-417, 10.5194/tc-16-397-2022, 2022.

https://doi.org/10.5194/egusphere-2026-669
Preprint. Discussion started: 2 March 2026

Wild, C. T., Kachuck, S. B., Luckman, A., Alley, K. E., Sharp, M. A., Smith, H., Tyler, S. W., Kratt, C., Dotto, T. S., Price, D., Nicholls, K. W., Bevan, S. L., Collao-Barrios, G., Muto, A., Truffer, M., Scambos, T. A., Heywood, K. J., and Pettit, E. C.: Rift propagation signals the last act of the Thwaites Eastern Ice Shelf despite low basal melt rates, Journal of Glaciology, 70, e21, 10.1017/jog.2024.64, 2024.

Williams, C., Trevers, M., Sun, S., Holland, P., Bett, D., Arthern, R., and Bradley, A.: Mass loss from Thwaites Glacier continues even without ocean melting, PREPRINT (Version 1) available at Research Square 10.21203/rs.3.rs-8660051/v1, 2026.

Williams, R. S. and Carter, W. D.: ERTS-1: a new window on our planet, 929, US Government Printing Office1976.

Yu, H., Rignot, E., Seroussi, H., and Morlighem, M.: Retreat of Thwaites Glacier, West Antarctica, over the next 100 years using various ice flow models, ice shelf melt scenarios and basal friction laws, The Cryosphere, 12, 3861-3876, 10.5194/tc-12-3861-2018, 2018.